applied sciences

MDPI

Article

Behavioral Analysis of an Interval Type-2 Fuzzy Controller Designed with Harmony Search Enhanced with Shadowed Type-2 Fuzzy Parameter Adaptation

Cinthia Peraza , Patricia Ochoa, Oscar Castillo * and Patricia Melin

Tijuana Institute of Technology, TecNM, Calzada Tecnologico s/n, Fracc. Tomas Aquino, Tijuana 22379, Mexico; cinthia.peraza@tectijuana.edu.mx (C.P.); martha.ochoa18@tectijuana.edu.mx (P.O.); pmelin@tectijuana.mx (P.M.)

* Correspondence: ocastillo@tectijuana.mx

Abstract: The challenges we face in today's world are increasingly complex, and effectively managing uncertainty when modeling control problems can yield significant benefits. However, the complexity of these models often leads to higher computational costs. Therefore, the main contribution of this article is the use of the theory of shadowed type-2 fuzzy sets to address these challenges and to control the search space exploration in the harmony search algorithm by employing two alpha planes, and with this, it was possible to reduce the computational cost and obtain effective results. Furthermore, the application of this approach aims to find optimal parameters for the membership functions of a type-2 fuzzy controller and analyze its behavior. By adopting the proposed methodology, it becomes possible to minimize computational costs while still achieving feasible solutions for interval type-2 control problems. A key aspect is that symmetry is considered in the design of the controller to also obtain good results. To validate the effectiveness of the approach, extensive simulations were conducted with varying levels of noise introduced to the type-2 controller. This comprehensive analysis allowed for a thorough examination of the results obtained. The findings of the simulations are presented, showcasing the advantages of the proposed methodology. By incorporating noise into the system, it was observed that the objective function, in this case, the root mean square error (RMSE), was reduced. Moreover, the signal obtained with the presence of noise demonstrated a superior performance compared to the noise-free reference. In conclusion, the proposed approach of utilizing shadowed type-2 fuzzy systems, combined with the harmony search algorithm, offers a promising solution for managing complex control problems. By carefully analyzing the behavior of the system through simulations, it is evident that the inclusion of noise helps improve the system's performance.

Keywords: interval type-2 shadowed sets; fuzzy controller; harmony search

check for updates

Citation: Peraza, C.; Ochoa, P.; Castillo, O.; Melin, P. Behavioral Analysis of an Interval Type-2 Fuzzy Controller Designed with Harmony Search Enhanced with Shadowed Type-2 Fuzzy Parameter Adaptation. *Appl. Sci.* **2023**, *13*, 7964. https://doi.org/10.3390/app13137964

Academic Editor: Andrea Prati

Received: 5 June 2023
Revised: 29 June 2023
Accepted: 4 July 2023
Published: 7 July 2023

Copyright: © 2023 by the authors. Licensee MDPI, Basel, Switzerland. This article is an open access article distributed under the terms and conditions of the Creative Commons Attribution (CC BY) license (https://creativecommons.org/licenses/by/4.0/).

1. Introduction

In recent years, a plethora of publications on control have appeared, and the analysis and design methods are important for a study carried out on control. Automatic control has emerged as a way to free workers from repetitive tasks, where the complexity of the system to be controlled is high, as there may be many reasons why automatic control is chosen. Manual control is carried out by people who know (even approximately) how to perform process control and understand how the control's outcome should be and how to achieve it. In an industry, these individuals (operators) have enough experience and knowledge to meet the control objectives. This concept of experience or a knowledge base is very important in fuzzy control systems: the objective of fuzzy logic control (FLC) systems is to control complex processes by means of human experience. Thus, fuzzy control systems and expert systems both stem from the same origins. However, their important differences should not be neglected. Whereas expert systems try to exploit uncertain knowledge acquired from an expert to support users in a certain domain, FLC systems, as we consider them here, are designed for the control of technical processes [1];

this paper reviews the studies on fuzzy control by referring to most of the papers written on fuzzy control. As an introduction, this paper picks up key points in applying fuzzy control and shows very recent results in industrial applications. This paper also points out some interesting and important problems to be solved [2], and it presents the first unified and thorough treatment of fuzzy modeling and fuzzy control, providing necessary tools for the control of complex nonlinear systems, based on three types of fuzzy models [3]. This paper presents a survey on recent developments of the analysis and design of fuzzy control systems focused on industrial applications reported after 2000 [4], and it reviews the key features of the above three types of fuzzy systems. Through these features, we point out the historical rationale for each type of fuzzy system and its current research mainstreams. However, the focus is put on fuzzy model-based approaches developed via the Lyapunov stability theorem and linear matrix inequality (LMI) formulations. Finally, our personal viewpoint on the perspectives and challenges of the future fuzzy control research is discussed [5]. The proposed HAGA model was applied to augment a T–S fuzzy controller that, in conjunction with the Fuzzy Clustering Mean (FCM), has enabled optimal rule generation and control parameter estimation. The proposed HAGA model exploits hierarchical concept-based AGA implementation that itself embodies novelties like an adaptive crossover and mutation probability, to enable accurate, swift, and efficient control function with the T–S fuzzy controller [6]. On this note, state-estimator-based adaptive control is under consideration for sort of nonlinear stochastic switched systems with the Takagi–Sugeno (T–S) fuzzy modeling and sliding mode technique. A new fuzzy sliding surface is established with a reformed state estimator, and novel adaptive fuzzy reaching motion controller synthesis is carried out to force the state trajectories onto the designated sliding surface in limited moments [7]. This paper studies the current sharing and voltage balancing problems of direct current microgrids (DC-MGs) consisting of distributed generation units (DGUs) connected by a communication network. The main challenge is that the DC-MG model is prone to unknown dynamic models and external disturbances [8], and this paper introduces a comprehensive review about the most recent advances in the design and implementation of type-2 fuzzy control schemes both for integer- and fractional-order systems [9]. In this article, an intelligent system utilizing type-3 fuzzy logic for automated image quality tuning in televisions is presented. The tuning problem can be formulated as controlling the television imaging system to achieve the requirements of production quality. Previously, the tuning process has been carried out by experts, by manually adjusting the television and imaging system on production lines to meet quality control standards [10].

The most prominent utilization of fuzzy logic is in the process of building controllers, which must generate outputs to act on certain mechanisms based on given inputs. The purpose of fuzzy controllers is simply to employ control strategies performed by human beings. Strategies in conventional PID (proportional integral derivative) control systems are expressed through mathematical functions, whereas systems based on fuzzy logic can more effectively control processes governed by intuitive rules that are difficult to express through complex mathematical constructs. Their great advantage lies in their ease of modification. Fuzzy control systems are the focus of interesting applications of fuzzy logic in the recent development of technological and industrial systems: an optimization approach is proposed to solve the problem that too many fuzzy control parameters are not easy to adjust. An MRMS composed of a ship model and a dual parallel elastic underactuated mooring robot is used to conduct experiments in terms of different motion-inhibition control methods [11], and this paper develops an event-triggered adaptive fuzzy control (AFC) scheme for stochastic nonlinear time-delay systems. With the aid of an event-triggered mechanism, the salient superiority involves reducing the data transmission and communication burden [12]. A type-2 fuzzy multi-objective evolutionary algorithm based on decomposition is used to optimize the proposed model and an adaptive large neighborhood search to enhance the local neighbor search mechanism. Additionally, by utilizing the nadir reference point, the distribution of Pareto front approximation is improved. Furthermore, a new metric is introduced to evaluate the dispersion of Pareto front approximation. The proposed method is compared to three other state-of-the-art evolutionary algorithms using 11 different performance metrics for validation [13]. Another paper presents the mitigation of subsynchronous resonance (SSR) based on a wide-area fuzzy controller in power systems including double-fed induction generator (DFIG)-based wind farms linked to series capacitive compensated transmission networks [14]. The proposed algorithm is employed to solve the problem based on routing associated with the time window for the heterogeneous fleet of the e-waste collection vehicle, and the approach is provided for the online system that enables people to request for the collection of e-waste components and also to solve the vehicle's routing problem. The optimization result demonstrates the decrease in the collection cost and the on-time e-waste collection from a household [15]. This paper contributes to command filtered adaptive fuzzy control (AFC) of fractional-order nonlinear systems (FNSs) by using the fractional backstepping control method. To approximate the virtual input, a fractional-order command filter (FCF) is proposed in [16]. A unified approach to fixed-time tracking control of stochastic high-order nonlinear systems (HONSs) with or without full-state constraints is studied in [17]. In this paper, to consider the running speed and stability of the manipulator, the time-optimal trajectory planning (TOTP) of the manipulator is transformed into a nonlinear optimal value search problem under multiple constraints, and a time-search algorithm based on fuzzy control is proposed, so that the end of the manipulator can run along the given path in Cartesian space for the shortest time, and the angular velocity and angular acceleration of each joint is within a limited range [18]. To begin with, a discrete LQR controller with feedforward and feedback components is designed based on the error model of vehicle lateral dynamics constructed by the natural coordinate system. Then, a fuzzy control method is applied to adjust the weight coefficients of the LQR in real time according to the state of the vehicle [19]. In another paper, an indirect hybrid solar-electric dryer was used to be able to dry a wide range of agriproducts and to ensure a continuous drying operation [20].

The shadowed type-2 fuzzy system (ST2-FHS) can be seen as an option to simplify fuzzy systems as they provide a solution by representing a fuzzy set based on two points (cuts), where the essential values are retained, and insignificant values are eliminated. The purpose of this approach is to minimize the issue of excessive precision in defining uncertainty. The aim of this work was to model a GT2 FLS based on shadowed type-2 fuzzy sets (ST2 FS) and apply this approach to control problems. The ST2 FS consists of approximating the secondary membership function with shadowed sets and it is because of this that we present an analytic approach to obtain the shadowed set for triangular and Gaussian membership functions for any parameters [21]. Traffic networks are getting big and complex day by day with a rapid traffic growth. Existing type-2 (T2) fuzzy logic works well in optimizing the waiting time of traffic at a big junction, but the rule base of T2 fuzzy logic is heavily dependent on previous traffic data, rather than real-time data. Moreover, it fails in changing and updating the waiting time in any junction with a high rate of traffic. In addition, very big junctions contain dynamic traffic data that are characterized by a high level of uncertainty, which is difficult to be handled with type-2 fuzzy logic. To cope with this situation, shadowed type-2 (ST2) fuzzy logic is proposed as it works well in a domain having very clumsy and uncertain data. It increases the uncertainty of a fuzzy set by partitioning it into a different region [22], and the ST2 FIS is based on the ideas of shadowed fuzzy sets and is an approximation of general type-2 fuzzy inference systems (GT2 FIS). The fundamental rationale for utilizing ST2 FIS instead of GT2 FIS is that the computational cost of GT2 FIS is too high for this application. The simulation results for the FTC using IT2 FIS and FTC using ST2 FIS for the Coupled Conical Tank Level Control (CCTLC) system with a 30% and 40% loss of effectiveness in the main actuator are presented in this study. In addition, this article compares the proposed FTC approach using ST2 FIS to FTC using IT2 FIS in terms of fault-recovery time [23]. This paper presents a novel methodology to obtain the shadowed set for all the secondary membership functions embedded in a general type-2 membership function. In this paper, we present an approach to obtain the shadowed set for a triangular and a Gaussian membership function. The idea is to model and perform a general type-2 fuzzy system based on shadowed type-2 fuzzy sets. The results are compared against the performance when a general-type fuzzy inference system is approximate when used on α-planes [24]. General type-2 fuzzy sets (GT2 FSs) have been originally proposed to allow for modeling uncertainty associated with the membership grades of type-1 (T1) FSs. However, because of the computational complexity associated with the processing of GT2 FSs, only their constrained version, the interval T2 (IT2) FSs, have been widely used. While IT2 FSs allow for fast processing, they lack the expressive power of GT2 FSs when modeling various kinds of uncertainties [25]. In this paper, the concept of a shadowed fuzzy set is introduced and some of its related operations are studied. A shadowed fuzzy set enables localization of the underlying uncertainty of fuzzy grades in type-2 fuzzy sets through exploitation of shadowed sets. It provides a capable framework that, despite preserving the uncertainties of fuzzy grades in type-2 fuzzy sets, adheres the simplicity of the concept and operations of interval type-2 fuzzy sets [26]. The use of the shadowed set theory is presented for parameter adaptation of the harmony search, which is inspired by music specifically in jazz improvisation. In this article, the goal was the optimization of an interval type-2 controller utilizing the variant of the harmony search with fuzzy adaptation. The study case with which the experimentation was carried out is a direct current motor, and its main characteristic is to maintain the stability of the motor position [27]; this paper suggests a better solution for such traffic issues via the delay-optimized Shortest Path Prediction (SPP) method. Even though shadowed type-2 (ST2) fuzzy logic works well for delay optimization with uncertain data, it causes a rise in fuzzy partitioning complexity [28]. The shadowed fuzzy set discussed in this paper provides a framework with a simplicity that is comparable with an interval type-2 fuzzy set but, on the other hand, preserves the fuzziness of the third dimension of type-2 fuzzy sets [29], and this study introduces a new concept of shadowed sets that can be regarded as a certain operational framework, simplifying processing carried out with the aid of fuzzy sets and enhancing interpretation of results obtained therein [30].

In [31–35], recent articles are presented where novel metaheuristics are used to solve various problems, which can be viewed as representative of the state of the art in this area.

The main contribution involves conducting a comprehensive behavioral analysis, utilizing an ST2-FHS for controlling the search space exploitation carried out by the harmony search, using two alpha planes in the approximation. Additionally, the application of this approach involves finding the parameter values of the membership functions in the design of a type-2 controller. Upon reviewing the existing literature, no similar work has been found, making this contribution significant.

This article is structured as follows: Section 2 provides the theory of fuzzy shadowed sets, while Section 3 presents the theoretical basis of the harmony search, as well as the description of the proposal. In Section 4, the use of shadowed fuzzy logic in the harmony search is discussed, and Section 5 contains the description and implementation of the controller. This is followed by Section 6, where simulations and an analysis of the results are outlined, and Section 7 offers the conclusions.

2. Shadowed Sets

Fuzzy logic has its beginnings in 1965 [36–38] and is primarily based on the understanding that our perception of the world cannot only be defined in terms of true or false statements. Instead, it is better to utilize concepts that can have a range of truth values within a set.

The evolution of fuzzy logic over time led to the development of different types of fuzzy systems. The first was the type-1 fuzzy system (T1-FS), followed by the interval type-2 fuzzy system (IT2-FS), and later the generalized type-2 fuzzy system (GT2-FS). The equations for these different fuzzy systems are presented as Equations (1)–(3), respectively:

$$\tilde{A} = \{(x, \mu_A(x))|x \in U, [0,1]\} \quad (1)$$

$$\tilde{A} = \{(x, u), u_{\tilde{A}}(x, u)|\forall x \in X, \forall u \in J_x \subseteq [0,1]\} \quad (2)$$

$$\tilde{\tilde{A}} = \left\{((x, u), \mu_{\tilde{A}}(x))\middle|\forall x \in X, \forall u \in J_x^u \subseteq [0,1]\right\} \quad (3)$$

The utilization of GT2-FS in real applications entails a high computational cost. However, there are alternative approaches to GT2-FS, such as vertical slices [39] and horizontal slices [40].

Therefore, this work focuses on the utilization of α-planes [22], as expressed by Equations (4) and (5) that describe the union of all α-planes.

$$\tilde{A}_\alpha = \{((x, u), \alpha)|\forall x \in X, \forall u \in J_x \subseteq [0,1]\} \quad (4)$$

$$\tilde{\tilde{A}} = \bigcup \tilde{A}_\alpha \quad (5)$$

ST2-FS [41] provides a solution to reduce computational costs. This work primarily focuses on modeling GT2-FS using only two α-planes, based on the theory proposed by Pedrycz for ST2-FS [42–44].

Equation (6) illustrates the mathematical manifestation of shadowed sets. This formula is constructed from two α-cuts on a T1-FS, incorporating α and β values, thereby defining three intervals.

$$S_{\mu_A}(x) = \begin{cases} 1, \text{ if } \mu_A(x) \geq \alpha \\ 0, \text{ if } \mu_A(x) \leq \beta \\ [0,1], \text{ if } \beta \leq \mu_A(x) \geq \alpha \end{cases} \quad (6)$$

Figure 1 illustrates the three regions of a shadowed set. The elevated area (EA) is represented by the blue color, with a membership of 1. The reduced area (RA) is depicted in yellow, with a membership of 0. The gray color represents the shadowed area (SA), which has a membership degree in the range of [0, 1].

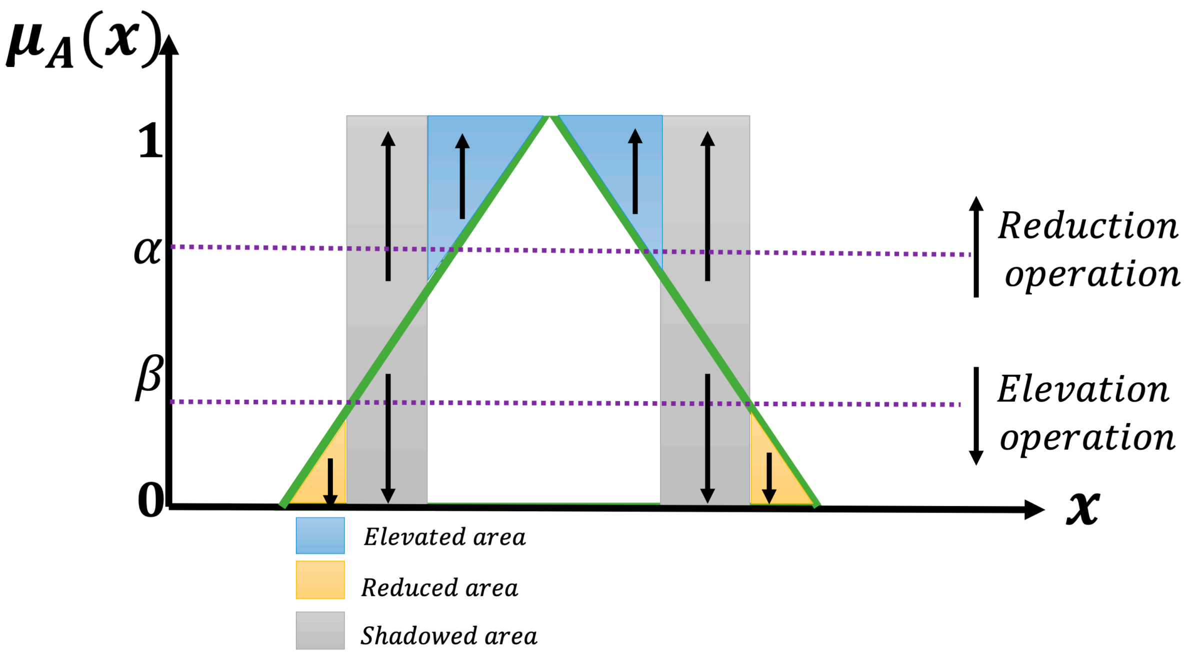

Figure 1. Representation of the shadowed set.

Taking these regions into consideration, Pedrycz proposed a method for calculating the optimal α and β values using Equation (7).

$$EA_{(\alpha,\beta)}(\mu_A) + RA_{(\alpha,\beta)}(\mu_A) = SA(\mu_A) \tag{7}$$

3. Harmony Search

The harmony search (HS), introduced by Prof. Geem [45], has been utilized from its inception in 2001 up to the present. The main inspiration behind HS is derived from music, specifically jazz improvisation. The algorithm incorporates three operations designed to mimic the behavior of a musician, which are mathematically described in Equations (8)–(10).

$$HMR \in [0, 1] \tag{8}$$

$$X_{new} = X_{old} + bp(2\ rand - 1) \tag{9}$$

$$PArate = P_{Lower\ limit} + P_{Range} \times rand Where\ P_{Range} = P_{Upper\ Limit} - P_{Lower\ Limit} \tag{10}$$

Equation (8) represents the first operation of the algorithm, which is like the playing of a piece that a musician knows by heart, also known as the memory acceptance rate (HMR). Equation (9) indicates the second operation, which resembles playing a piece and adjusting the tones, known as pitch adjustment (PArate). Finally, Equation (10) represents the action of playing a new piece and randomly adjusting the notes, also known as random selection.

Further details on the behavior of each operator can be found in the following articles [46–48]. Algorithm 1 consists of the pseudocode for HS and Figure 2 shows the HS flowchart.

Algorithm 1: HS

1. State the objective function $f(x), x = (X_1, \ldots, X_n)^T$
2. Initially generate harmonics (matrix of real numbers)
3. Establish the pitch adjustment rate (PArate) and limits of tone
4. Establish harmony memory accepting (HMR)
5. While (t < Maximum number of iterations)
6. Produce a new harmony and accept the best system
7. Setting the tone for new harmonies (solutions)
8. If (rand > HMR)
9. Randomly select an existing harmony
10. Else if (rand > PArate)
11. Setting the tone at random within a bandwidth
12. Else
13. Produce a new harmony through a randomization
14. End if
15. Accepting new harmonies (solutions) best
16. End while
17. Find the best solutions

The most recent articles found in the literature regarding HS report applications to real problems in various disciplines. The applications are as follows: healthcare systems [49], scheduling problems [50], optimization problems such as a seismic isolator [51], ground motion [52], a pre-stressed concrete bridge girder [53], and Distribution Network Reconfiguration [54]. Furthermore, some of the more recent variants of the algorithm are presented in [55,56].

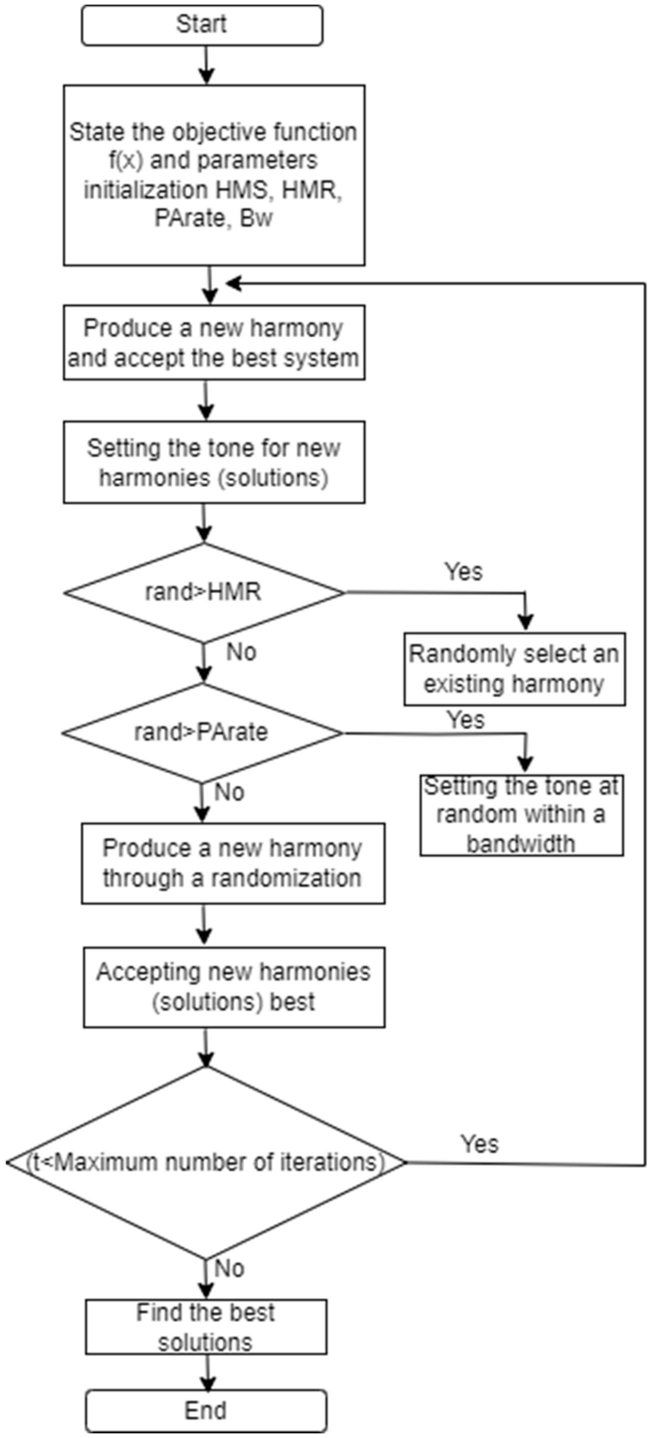

Figure 2. Representation of the HS algorithm.

4. Proposed Shadowed Fuzzy System Using HS Algorithm

In this section, we provide a description of the structure of the fuzzy system employed for the experimental analysis. This fuzzy system, referred to as SFHSA (shadowed fuzzy harmony search algorithm), is depicted in more detail in Figure 3, providing a visual representation of its components and structure.

SFHSA serves as the framework for integrating the ST2-FHS approach into the optimal type-2 fuzzy controller design. It effectively manages the harmonization process, enabling efficient search space exploration and exploitation. The utilization of shadow sets and the incorporation of two alpha planes play crucial roles in enhancing the performance of the algorithm, which can be viewed as the key contribution of this work.

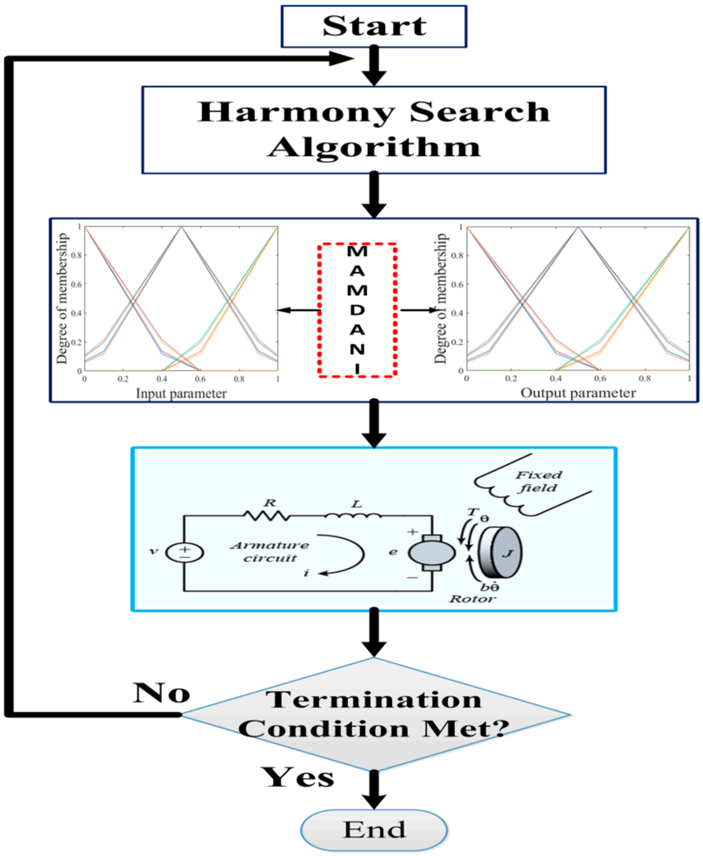

Figure 3. Diagram of the main proposal.

Figure 3 offers a comprehensive illustration of the SFHSA structure, allowing for a clear understanding of its key components and their interconnections. This diagram serves as a visual aid to facilitate the comprehension of the algorithm's implementation and its information flow.

By employing the SFHSA methodology, this article aimed to address the challenges associated with optimizing the parameters of the membership functions in an interval type-2 fuzzy controller. The proposed approach not only enhances the computational efficiency but also ensures the attainment of more effective and accurate control outcomes.

The subsequent sections of this article will delve into the experimental results obtained using SFHSA and present a comprehensive analysis of its performance. These findings will shed light on the effectiveness and reliability of the proposed methodology in addressing the control challenges associated with type-2 fuzzy systems.

Equations (11) and (12) represent the calculation of the input and output of the SFHSA.

$$\text{Iteration} = \frac{\text{Current Iteration}}{\text{Maximun of iterations}} \tag{11}$$

$$\text{HMR} = \frac{\sum_{i=1}^{r_{hmr}} \mu_i^{hmr}(hmr_{1i})}{\sum_{i=1}^{r_{hmr}} \mu_i^{hmr}} \tag{12}$$

In these equations, HMR represents the memory consideration, r_{hmr} denotes the number of rules in the SFHSA corresponding to HMR, hmr_{1i} represents the output result for rule i corresponding to HMR, and μ_i^{hmr} represents the membership function of rule i corresponding to HMR.

Algorithm 2 depicts the pseudocode of the enhanced SFHSA with parameter adaptation and Figure 4 shows the SFHSA flowchart.

Algorithm 2: SFHSA

```
Define objective function f(x), x = (X_1, ..., X_n)^T
Initially generate harmonics (matrix of real numbers)
Establish the pitch adjustment rate (PArate) and limits of tone
Establish the harmony memory accepting (HMR)
While (t < Maximum number of iterations)
    Calculate iteration using Equation (11)
    Calculate new HMR parameter using a SFHSA fuzzy system of Equation (12)
    Produce a new harmony and accept the best system
    Setting the tone for new harmonies (solutions)
    If (rand > HMR)
        Randomly select an existing harmony
    Else if (rand > PArate)
        Setting the tone at random within a bandwidth
    Else
        Produce a new harmony through a randomization
    End if
Accepting new harmonies (solutions) best
End while
Find the best solutions
```

The design of SFHSA consists of a Mamdani-type system, which includes an input named "Iteration." This input is characterized by three membership functions (MFs) called "Small", "Medium", and "Big".

The output of the SFHSA system is represented by the HMR parameter, which is defined by three MFs: "Small", "Medium", and "Big". Figure 5 illustrates the structure of SFHSA.

The SFHSA rules were developed incrementally, and they were created based on previous experimentation. It was observed that starting with a high HMR parameter and gradually decreasing it during the iterations leads to better results. Table 1 illustrates the behavior of the SFHSA rules.

Table 1. Rules of the SFHSA.

HMR Iteration	Small	Medium	Big
Small	Small	–	–
Medium	–	Medium	–
Big	–	–	Big

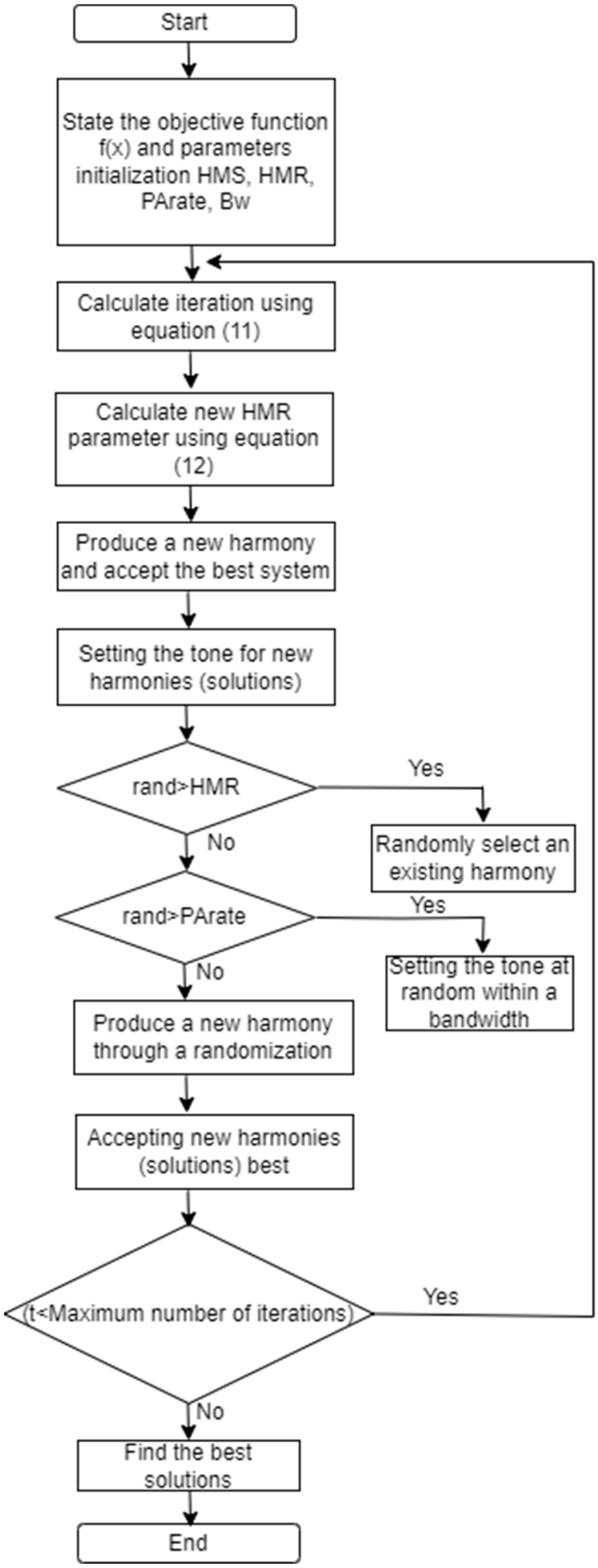

Figure 4. Illustration of the SFHSA flowchart.

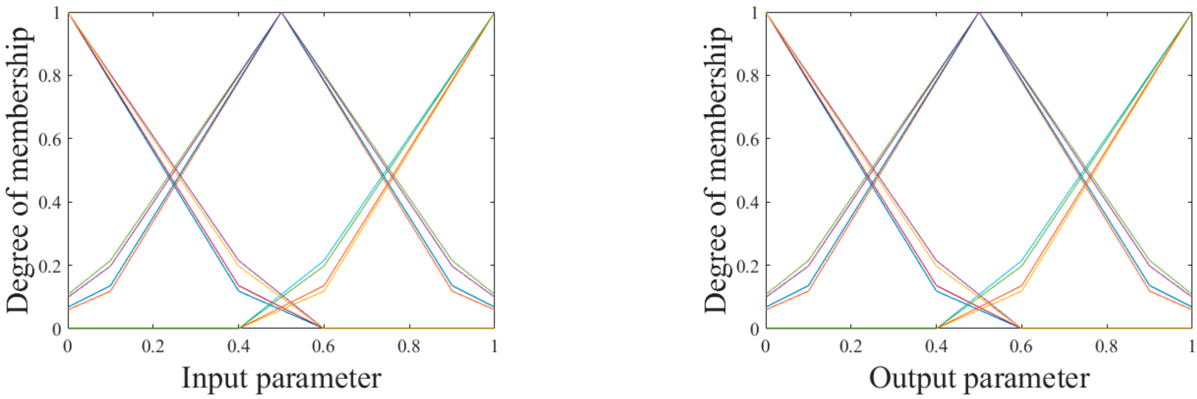

Figure 5. Structure of the SFHSA.

5. Interval Type-2 Controller of Motor Angular Position

For the experimental phase of this study, we deemed it appropriate to focus on a widely recognized benchmark control problem, specifically the Motor Angular Position Controller (IT2FLC-MAP). This particular problem serves as an excellent testbed for evaluating the performance and effectiveness of the proposed methodology.

To provide a visual representation of the IT2FLC-MAP, Figure 6 presents a graphical illustration that elucidates the key aspects and dynamics of the control problem. This representation helps in understanding the intricate relationship between the control inputs and the output; we assume that the input of the system is the voltage source (v) applied to the motor's armature, which represents the manipulated variable, while the output is the position of the shaft (θ), which represents the controlled variable.

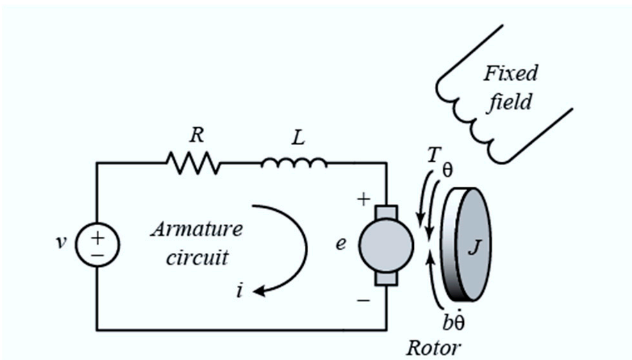

Figure 6. Graphical representation of the IT2FLC-MAP.

In addition to the graphical representation, the mathematical model of the IT2FLC-MAP is provided in Equations (13) and (14). These equations contain the underlying principles and relationships governing the control problem, allowing for a comprehensive understanding of its dynamics.

To facilitate the implementation and evaluation of the methodology, Table 2 outlines the configuration of the controller variables used in the IT2FLC-MAP. These variables play a crucial role in defining the behavior and performance of the controller, enabling effective control over the motor's angular position.

By considering the well-known IT2FLC-MAP as the basis for experimentation, this study aimed to provide an evaluation of the methodology's capabilities and performance. The mathematical model, graphical representation, and controller variable configuration collectively form the foundation for performing the experimental analysis.

Table 2. Configuration of the controller variables.

Parameter	Description	Value
J	Inertia of the rotor	3.2284×10^{-6} kg.m^2
b	Viscous friction	3.5077×10^{-6} Nms
Ke	Electromotive force	0.0274 V/rad/s
Kt	Torque constant	0.0274 Nm/Amp
R	Electric resistance	4 ohms
L	Electric inductance	2.75×10^{-6} H

In the subsequent sections, we will delve into the experimental results obtained using the IT2FLC-MAP and assess the performance of the methodology in addressing the control challenges associated with this specific benchmark problem. These findings will contribute to our understanding of the effectiveness and applicability of the approach in real-world control scenarios.

$$\frac{d}{dt}\begin{bmatrix}\theta \\ \dot{\theta} \\ i\end{bmatrix} = \begin{bmatrix} 0 & 1 & 0 \\ 0 & -\frac{b}{J} & \frac{K}{J} \\ 0 & -\frac{K}{L} & -\frac{R}{L} \end{bmatrix}\begin{bmatrix}\theta \\ \dot{\theta} \\ i\end{bmatrix} + \begin{bmatrix}0 \\ 0 \\ \frac{1}{L}\end{bmatrix} \tag{13}$$

$$y = \begin{bmatrix}1 & 0 & 0\end{bmatrix}\begin{bmatrix}\theta \\ \dot{\theta} \\ i\end{bmatrix} \tag{14}$$

The interval type-2 fuzzy logic controller (IT2FLC), which is represented in Figure 7, implemented to analyze the behavior of the proposed method is composed of interval type-2 MFs (IT2MFs), which are mathematically formulated with Equations (15) and (16).

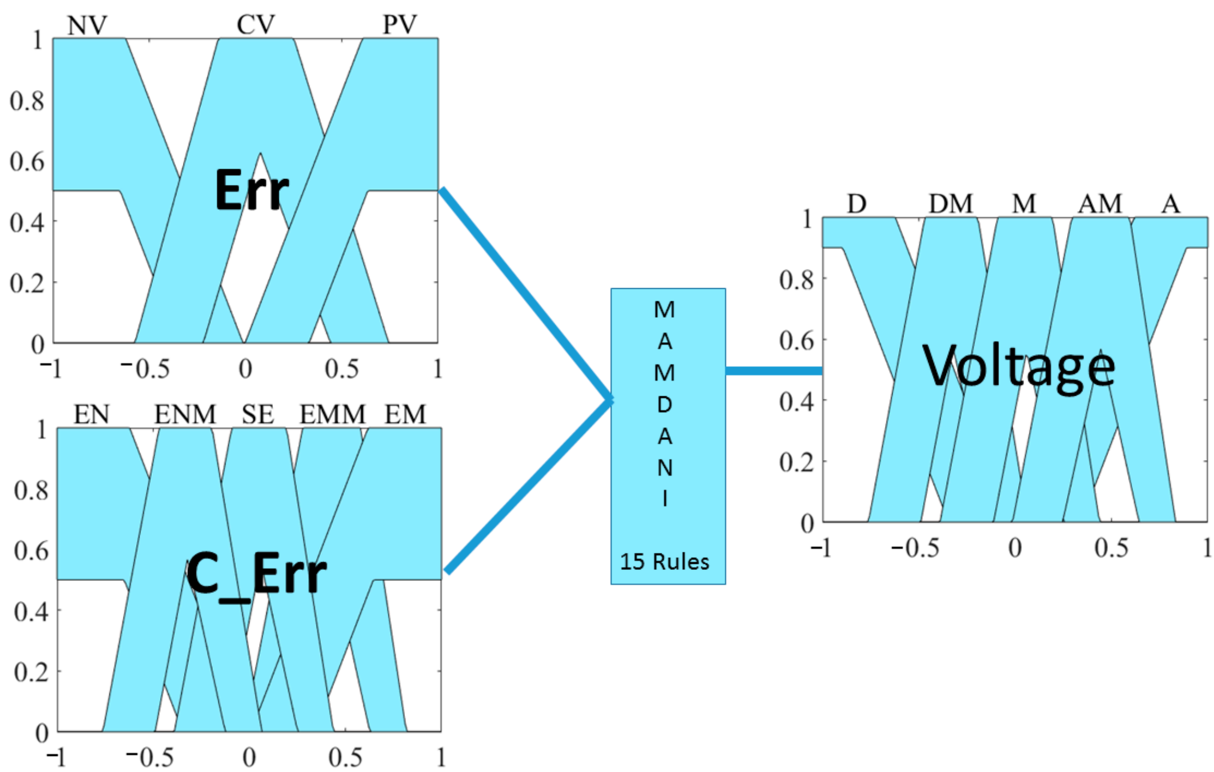

Figure 7. IT2FLC structure for the IT2FLC-MAP.

The values used for the IT2MF of the IT2FLC are presented in Table 3, while Table 4 expresses the behavior of the rules of the IT2FLC-MAP.

$$\text{trapeIT2mf} = \begin{cases} e_1 < e_2, f_1 < f_2, g_1 < g_2, h_1 < h_2 \\ \mu_1(x) = \max\left(\min\left(\frac{x-e_1}{f_1-e_1}, 1, \frac{h_1-x}{h_1-g_1}\right), 0\right) \\ \mu_2(x) = \max\left(\min\left(\frac{x-e_2}{f_2-e_2}, 1, \frac{h_2-x}{h_2-g_2}\right), 0\right) \\ \mu(x) = \begin{cases} \max(\mu_1(x), \mu_2(x)) & \forall x \notin (f1, g2) \\ 1 & \forall x \in (f1, g2) \end{cases} \\ \underline{\mu}(x) = \min(\alpha, \min(\mu_1(x), \mu_2(x))) \end{cases} \quad (15)$$

$$\text{triaIT2mf} = \begin{cases} e_1 < e_2, f_1 < f_2, g_1 < g_2 \\ \mu_1(x) = \max\left(\min\left(\frac{x-e_1}{f_1-e_1}, \frac{g_1-x}{g_1-f_1}\right), 0\right) \\ \mu_2(x) = \max\left(\min\left(\frac{x-e_2}{f_2-e_2}, \frac{g_2-x}{g_2-f_2}\right), 0\right) \\ \mu(x) = \begin{cases} \max(\mu_1(x), \mu_2(x)) & \forall x \notin (f1, f2) \\ 1 & \forall x \in (f1, f2) \end{cases} \\ \underline{\mu}(x) = \min(\mu_1(x), \mu_2(x)) \end{cases} \quad (16)$$

Table 3. IT2MF.

Input Err								
IT2MF	e1	f1	g1	h1	e2	f2	g2	h2
NVol	−1.9	−1.3	−0.9	−0.3	−1.6	−1.0	−0.6	0
ZeroV	−0.5	−0.1	0.28	---	−0.2	0	0.5	---
PVol	0	0.5	1.0	1.6	0.3	0.9	1.3	1.9
Input C_Err								
ENeg	−1.6	−1.0	−0.6	−0.2	−1.3	−0.7	−0.3	0
ENMax	−0.4	−0.2	0	---	−0.2	0	0	---
SE	−0.1	0	0	---	0	0	0.1	---
EMMax	0	0.1	0.3	---	0.1	0.2	0.4	---
EMax	0.3	0.7	0.7	1.1	0	0.4	1.2	1.2
Output Voltage								
D	−1.8	−1.4	−0.8	−0.2	−1.6	−1.2	−0.6	0
DM	−0.4	−0.2	−0.1	---	−0.3	−0.2	0	---
M	−0.1	0	0	---	0	0	0.1	---
AM	0	0.1	0.3	---	0.1	0.2	0.4	---
A	0.1	0.5	1.1	1.5	0.3	0.7	1.3	1.7

Table 4. IT2FLC rules of IT2FLC-MAP.

Rule Number	**Inputs**		**Output**
	Err	C_Err	Voltage
1	NVol	ENeg	D
2	NVol	SE	D
3	NVol	EMax	DM
4	ZeroV	ENeg	AM
5	ZeroV	EMax	DM
6	PVol	ENeg	AM
7	PVol	SE	A
8	PVol	EMax	A
9	ZeroV	SE	M
10	NVol	ENMax	D
11	ZeroV	ENMax	AM
12	PVol	ENMax	A
13	PVol	EMMax	A
14	ZeroV	EMMax	DM
15	NVol	EMMax	D

Figure 8 illustrates the surface of the IT2FLC for the IT2FLC-MAP, while Figure 9 represents the reference for the IT2FLC-MAP.

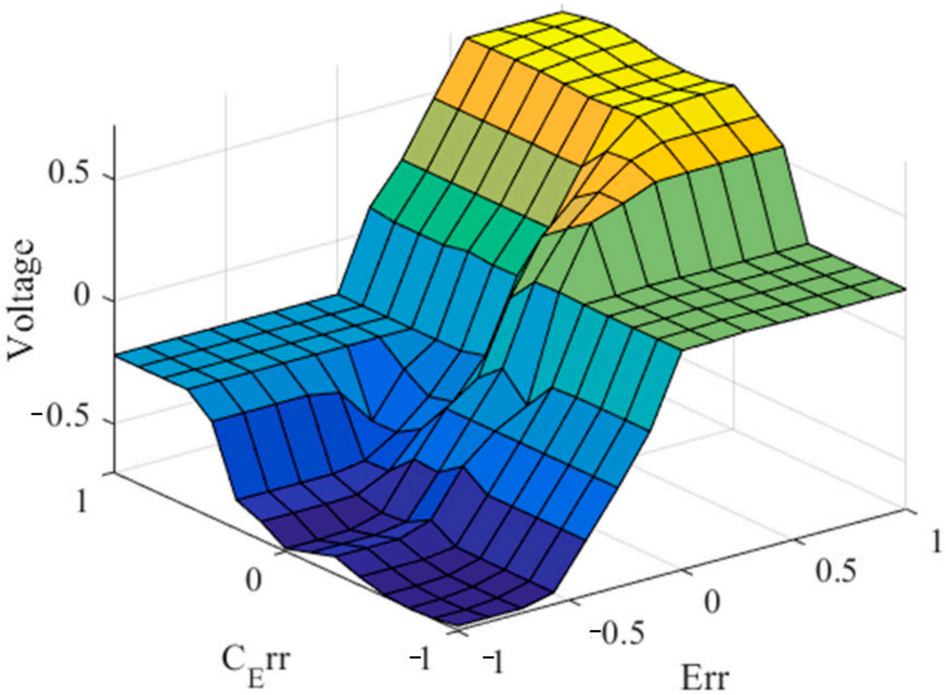

Figure 8. Surface of the IT2FLC for the IT2FLC-MAP.

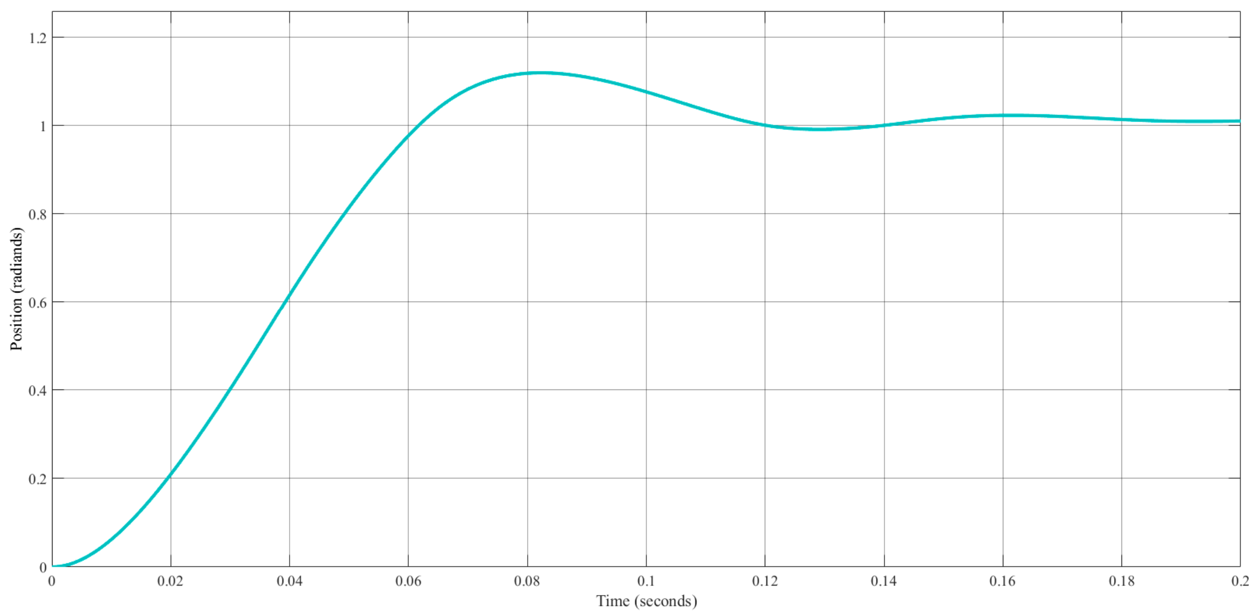

Figure 9. Reference for the IT2FLC-MAP.

6. Simulation Results

To thoroughly assess the performance of the SFHSA method, a series of simulations were performed. These simulations were divided into two distinct case studies, each aimed at investigating the behavior of the controller under different conditions.

In the first case study, the proposed controller IT2FLC was evaluated without the addition of any noise. This allowed for a baseline evaluation of the controller's performance in a noise-free environment.

The second case study involved the application of various levels of uniform random number noise (URN) to the controller. This approach allowed for a comprehensive analysis of the controller's robustness and adaptability in the presence of noise. The simulations were carried out using nine different noise levels, ranging from 0.01 to 0.09.

To evaluate the efficiency of the IT2FLC, the SFHSA algorithm was employed. The simulations were configured with specific parameters, including a PArate of 0.75, 35 harmonies, 30 simulations, and 100 iterations. These settings ensured a thorough exploration of the search space and provided reliable results for performance evaluation.

In the experiments, the performance indices, represented by Equations (17)–(22), were utilized to assess the controller's effectiveness. However, the primary objective function focused on minimizing the Root Mean Square Error (RMSE), which served as a reliable measure of the controller's performance in accurately tracking the desired output.

By considering the performance indices and the objective function, a comprehensive evaluation of the controller's performance under different noise levels was conducted. This analysis allowed for a detailed understanding of how the controller responded to varying levels of noise and provided insights into its adaptability and robustness in uncertain environments.

The results obtained from these simulations, along with the corresponding performance indices, will be presented and discussed in subsequent sections. These findings will contribute to the overall understanding of the proposed method and provide valuable insights for further improvements in control system design.

Overall, the simulation studies conducted with and without noise provided valuable data for evaluating the efficiency and robustness of the SFHSA-based controller. The analysis of the performance indices and the focus on minimizing RMSE ensured a comprehensive assessment of the controller's performance under different conditions.

$$\mathrm{MSE} = \frac{1}{n}\sum_{i=1}^{n}\left(\overline{Y}_i - Y_i\right)^2 \tag{17}$$

$$\mathrm{RMSE} = \sqrt{\frac{1}{N}\sum_{t=1}^{N}(x_t - \hat{x}_t)^2} \tag{18}$$

$$\mathrm{ITAE} = \sum_{t=1}^{N} t(x(t) - \hat{x}(t)) \tag{19}$$

$$\mathrm{IAE} = \sum_{t=1}^{N}|x(t) - \hat{x}(t)| \tag{20}$$

$$\mathrm{ITSE} = \sum_{t=1}^{N} t\left(\left(x(t) - \hat{x}(t)\right)^2\right) \tag{21}$$

$$\mathrm{ISE} = \sum_{t=1}^{N}\left|\left(x(t) - \hat{x}(t)\right)^2\right| \tag{22}$$

The results of the performance index obtained from the 30 simulations are outlined in Table 5. This table displays the values obtained without noise and with noise for the proposed controller. It can be noted that adding uncertainty to the controller significantly improves its performance.

Tables 6–8 present the performance index obtained by varying the URN noise level in the proposed controller. The best result is achieved when a noise level of 0.01 is applied to the controller. As the noise level increases, the RMSE results follow the same order. Therefore, introducing uncertainty to the controller enhances its performance.

Table 5. Results without URN noise and with URN noise in the IT2FLC controller.

Performance Index	ST2FHS without URN Noise	ST2FHS with URN Noise
MSE	6.52×10^{-1}	6.28×10^{-1}
RMSE	8.07×10^{-1}	7.92×10^{-1}
ITAE	1.98×10^{-2}	1.95×10^{-2}
IAE	1.71×10^{-1}	1.68×10^{-1}
ITSE	2.01×10^{-2}	1.95×10^{-2}
ISE	1.68×10^{-1}	1.62×10^{-1}

Table 6. Results with 0.01, 0.02, 0.03, and 0.04 URN noise levels in the IT2FLC controller.

Performance Index	0.01 URN	0.02 URN	0.03 URN	0.04 URN
MSE	6.73×10^{-1}	6.69×10^{-1}	6.61×10^{-1}	6.52×10^{-1}
RMSE	2.88×10^{-2}	3.10×10^{-2}	3.07×10^{-2}	3.35×10^{-2}
ITAE	2.01×10^{-2}	2.01×10^{-2}	2.00×10^{-2}	1.98×10^{-2}
IAE	1.74×10^{-1}	1.73×10^{-1}	1.72×10^{-1}	1.71×10^{-1}
ITSE	2.07×10^{-2}	2.05×10^{-2}	2.03×10^{-2}	2.01×10^{-2}
ISE	1.72×10^{-1}	1.72×10^{-1}	1.70×10^{-1}	1.71×10^{-1}

Table 7. Results with 0.05, 0.06, 0.07, and 0.08 URN noise levels in the IT2FLC controller.

Performance Index	0.05 URN	0.06 URN	0.07 URN	0.08 URN
MSE	6.28×10^{-1}	6.33×10^{-1}	6.26×10^{-1}	6.18×10^{-1}
RMSE	3.46×10^{-2}	3.57×10^{-2}	3.46×10^{-2}	3.41×10^{-2}
ITAE	1.95×10^{-2}	1.96×10^{-2}	1.95×10^{-2}	1.93×10^{-2}
IAE	1.68×10^{-1}	1.69×10^{-1}	1.68×10^{-1}	1.67×10^{-1}
ITSE	1.95×10^{-2}	1.96×10^{-2}	1.94×10^{-2}	1.91×10^{-2}
ISE	1.62×10^{-1}	1.63×10^{-1}	1.62×10^{-1}	1.60×10^{-1}

Table 8. Results with 0.09 URN noise level in the IT2FLC controller.

Performance Index	0.09 URN
MSE	6.16×10^{-1}
RMSE	3.42×10^{-2}
ITAE	1.93×10^{-2}
IAE	1.67×10^{-1}
ITSE	1.90×10^{-2}
ISE	1.59×10^{-1}

Table 9 shows the average time of 30 runs with each noise level applied to the experimentation of the IT2FLC controller.

Table 9. Experiment time with each URN noise level in the IT2FLC controller.

Level of URN Noise	Time (Seconds)
Without URN noise	640.50
0.01	661.12
0.02	644.44
0.03	650.40
0.04	645.90
0.05	649.50
0.06	645.00
0.07	429.20
0.08	647.40
0.09	659.40

With this, it is demonstrated that a reduction in time is achieved with the proposed methodology using only two alpha planes by increasing the complexity of the problem, and by converting the interval type-2 fuzzy controller, it is possible to manage uncertainty and maintain the objective of the controller while increasing noise levels.

When comparing the results obtained in this article with others existing in the literature, as shown in [27], we can observe that the error when applying a noise level of 0.5 results in an error of 2.10×10^{-3} and, with this proposal, a noise level of 3.46×10^{-2} is obtained; therefore, there is closeness between the errors, and it is important to highlight that, even so, the objective of the controller is maintained for a considerable time when using the proposed methodology.

Figures 10–27 display the reference and surface obtained from the simulation conducted with varying URN noise levels in the controller, ranging from 0.01 to 0.09.

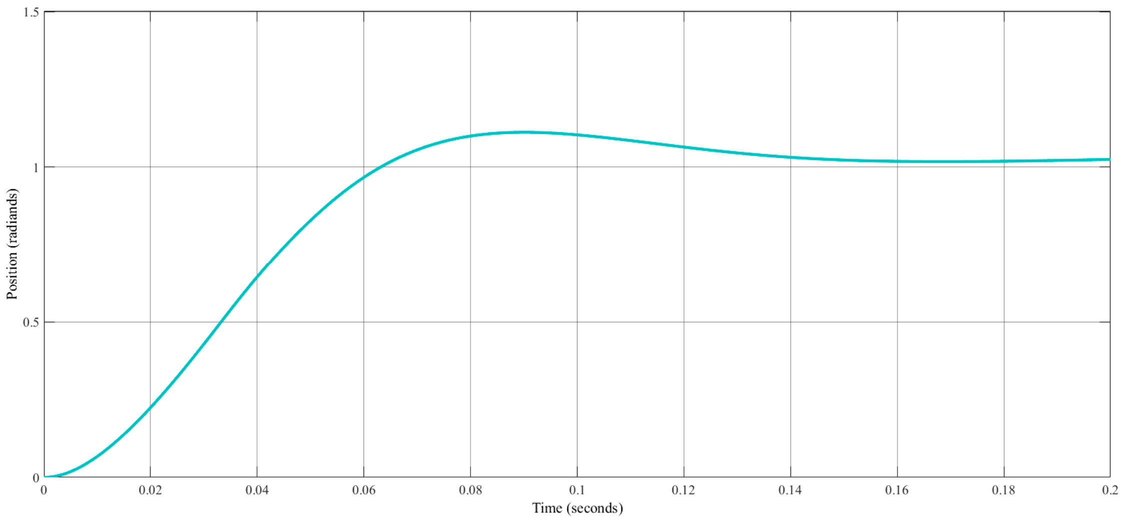

Figure 10. Controller reference using 0.01 URN noise.

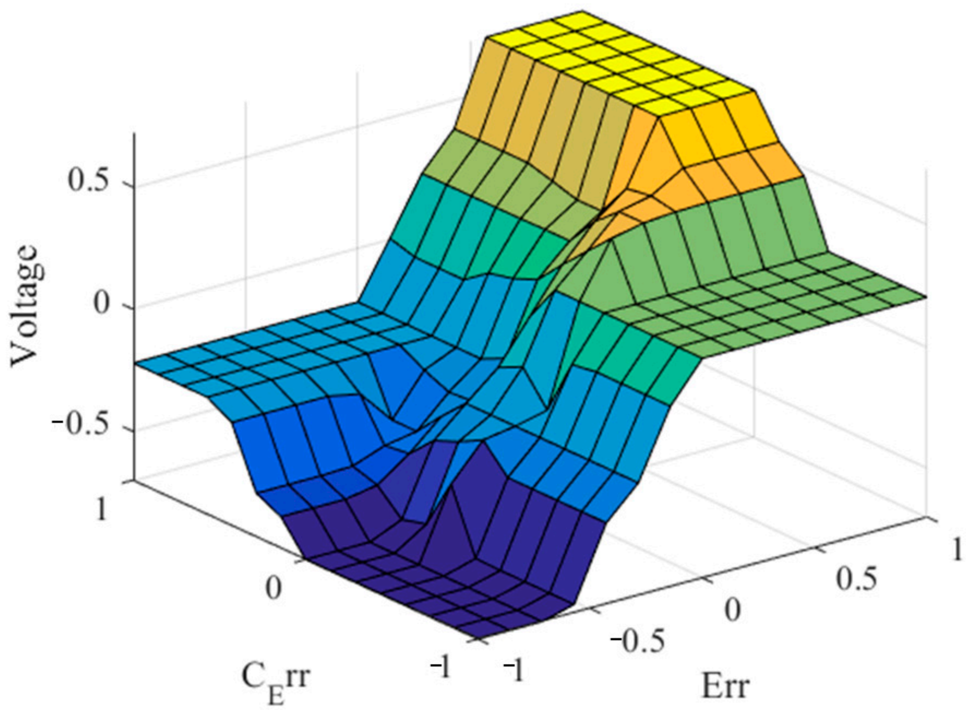

Figure 11. Surface using 0.01 URN noise.

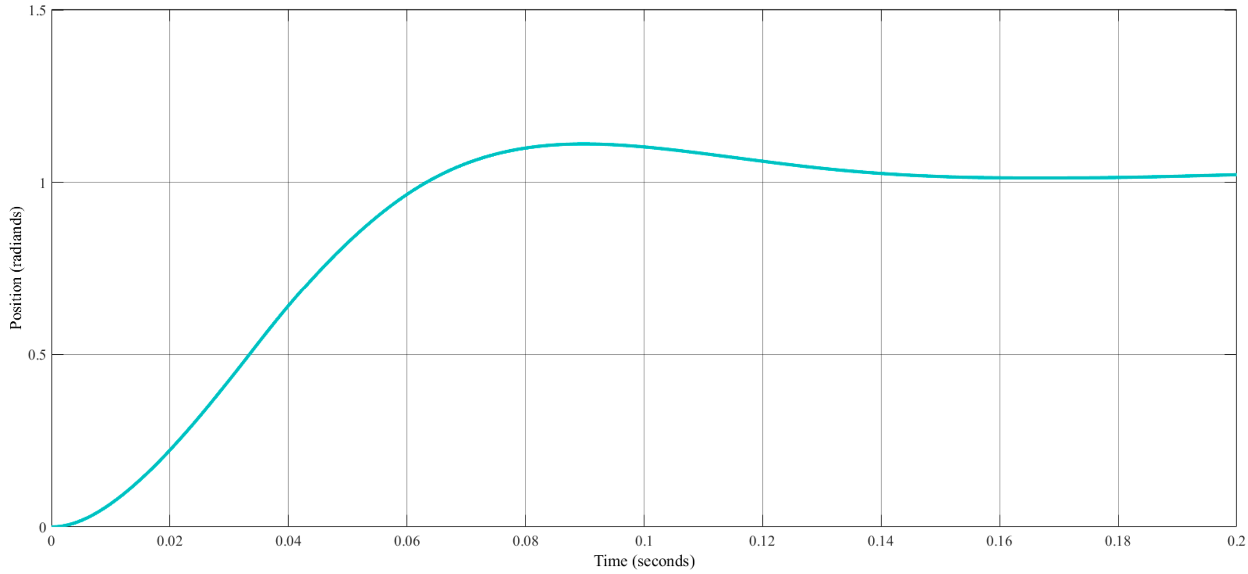

Figure 12. Controller reference using 0.02 URN noise.

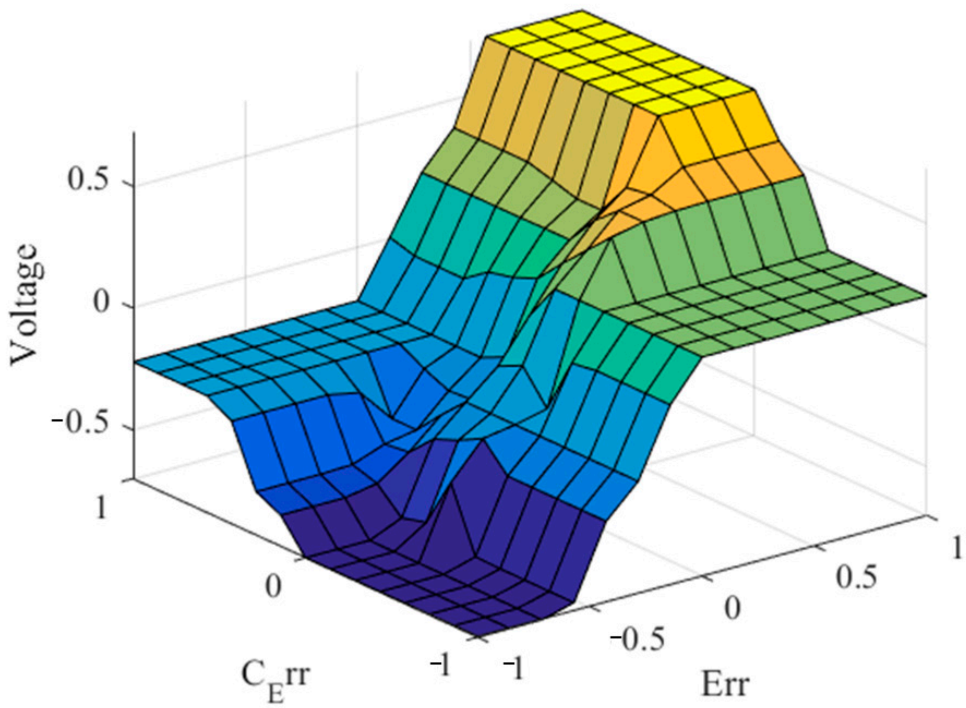

Figure 13. Surface using 0.02 URN noise.

Upon a thorough analysis of the results presented in Figures 10–27, it can be seen that the controller is stable between 0.14 and 0.15 s and, when applying different noise levels, a clear pattern emerges: as the noise level in the controller increases, so does the level of uncertainty. Simultaneously, the objective function maintains a consistent order throughout the simulations. This observation provides strong evidence to support the effectiveness of the proposed approach in managing uncertainty.

The progressive increase in the noise level serves as a deliberate manipulation to introduce more uncertainty into the system. By doing so, the robustness and adaptability of the controller are tested and evaluated. The results consistently demonstrate that as the noise level rises, the controller successfully handles the increased uncertainty without compromising the objective function.

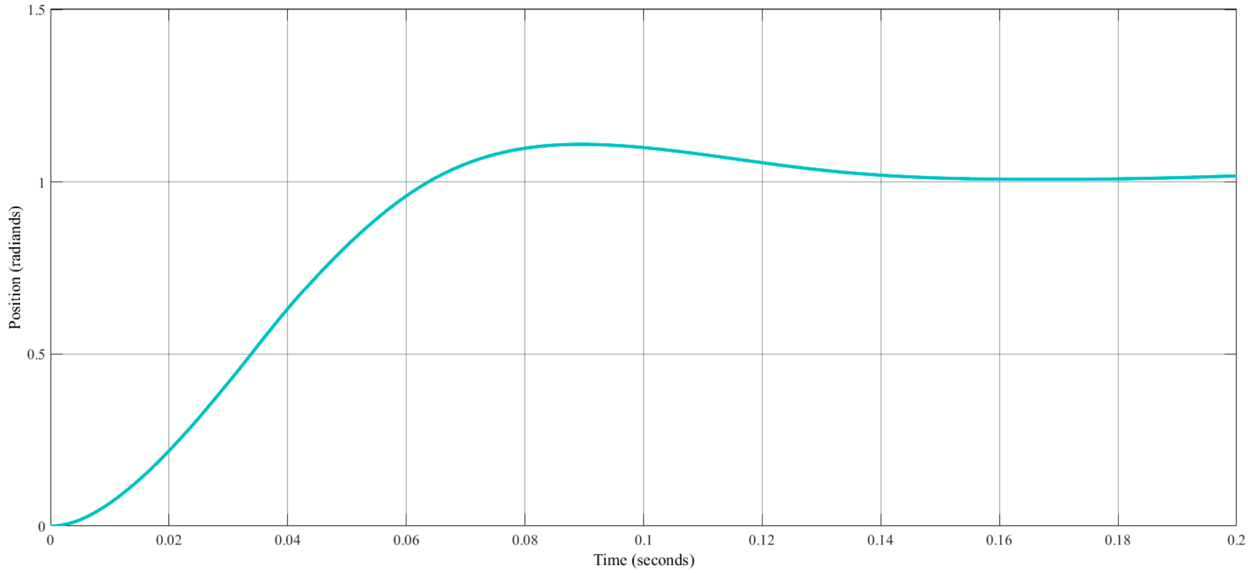

Figure 14. Controller reference using 0.03 URN noise.

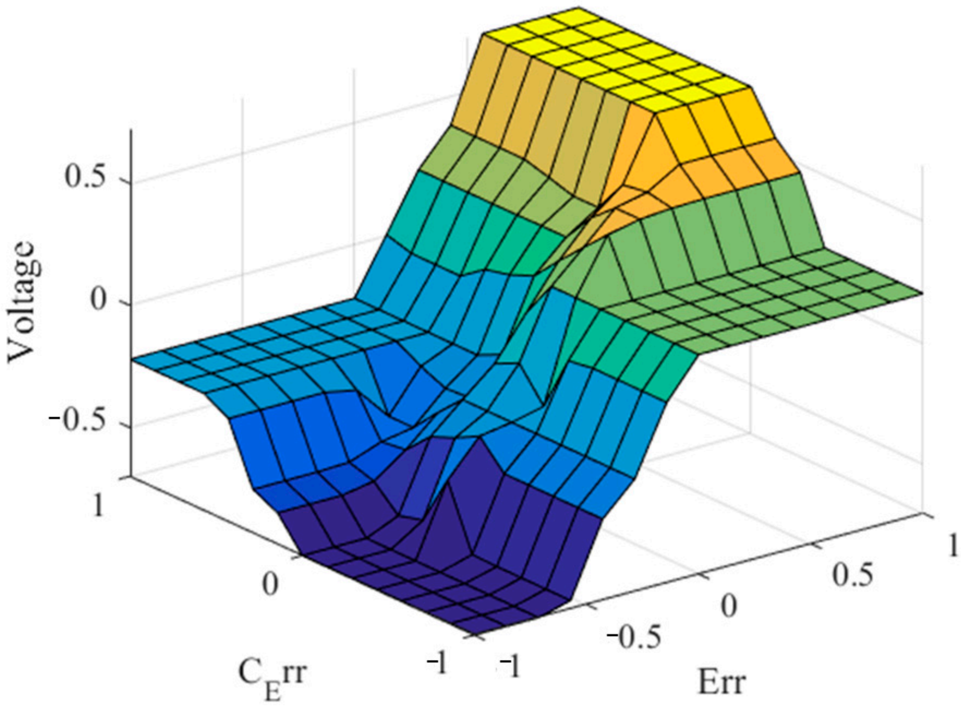

Figure 15. Surface using 0.03 URN noise.

These findings have significant implications for control systems, particularly in complex and dynamic environments where uncertainty is prevalent. The proposed approach showcases its ability to effectively handle and mitigate uncertainty, ensuring a reliable performance even in the presence of noise. This is crucial for real-world applications where unpredictable factors and disturbances can significantly impact system behavior.

The results presented in the figures vividly illustrate the performance of the controller under different noise levels. The comparison between the obtained signals and the noise-free reference clearly shows the superior performance achieved when noise is introduced. This improvement in the performance substantiates the claim that adding uncertainty to the controller can yield better results.

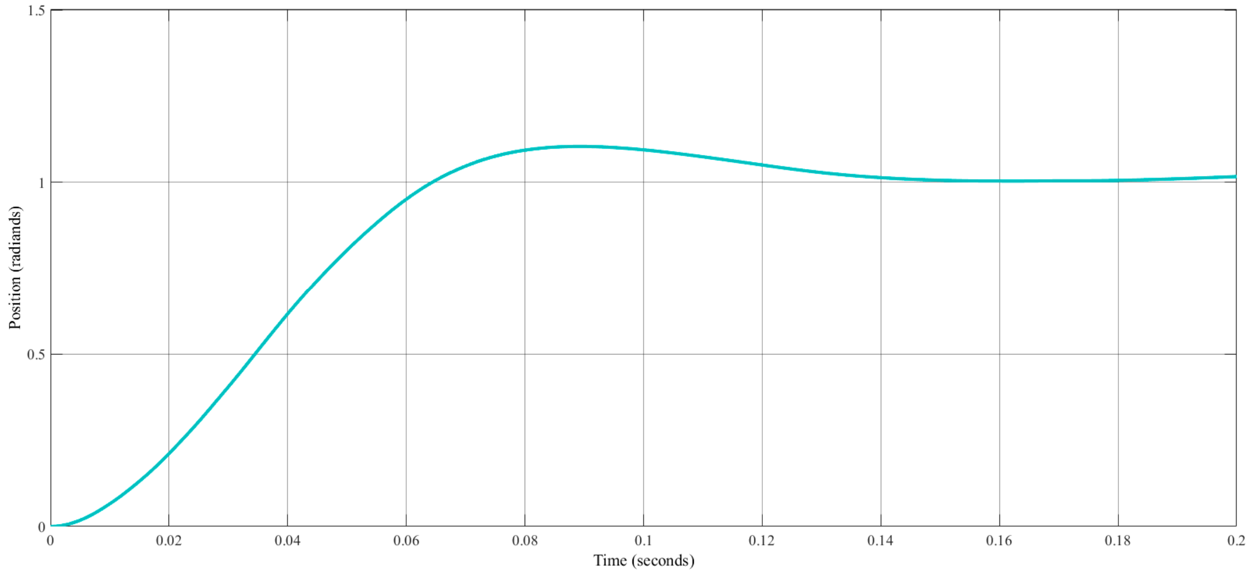

Figure 16. Controller reference using 0.04 URN noise.

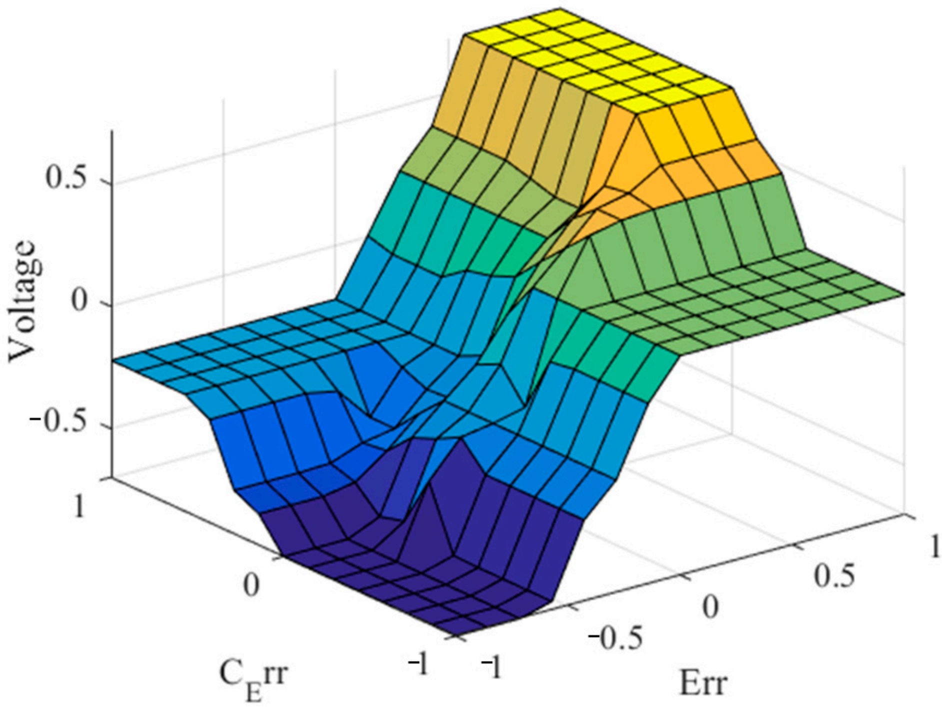

Figure 17. Surface using 0.04 URN noise.

In conclusion, the comprehensive analysis of the simulation results highlights the effectiveness of the proposed approach in managing uncertainty. The observed relationship between the increasing noise level, the corresponding increase in controller uncertainty, and the consistent order of the objective function provides strong validation for the proposed methodology. These findings contribute to the advancement of control system design by offering a robust solution to address uncertainty in complex environments.

Further research endeavors may explore the application of type-3 fuzzy controllers or extend the proposed methodology to different control problem domains. By continuing to explore and refine the proposed approach, control systems can be further enhanced to tackle increasingly complex challenges in various industries and domains.

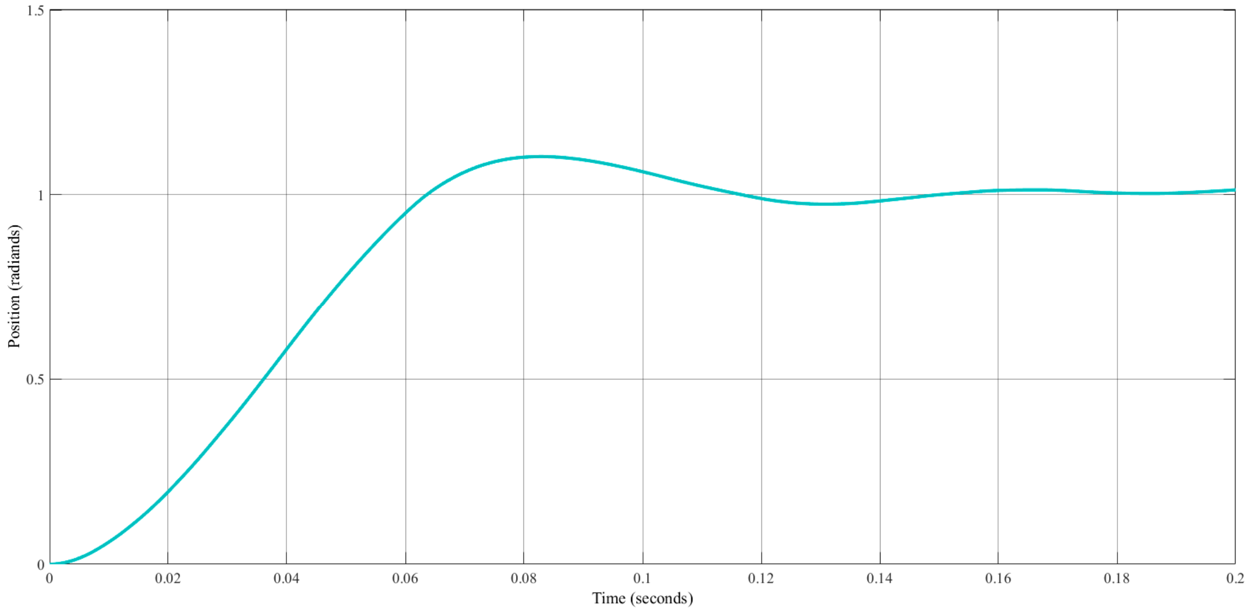

Figure 18. Controller reference using 0.05 noise.

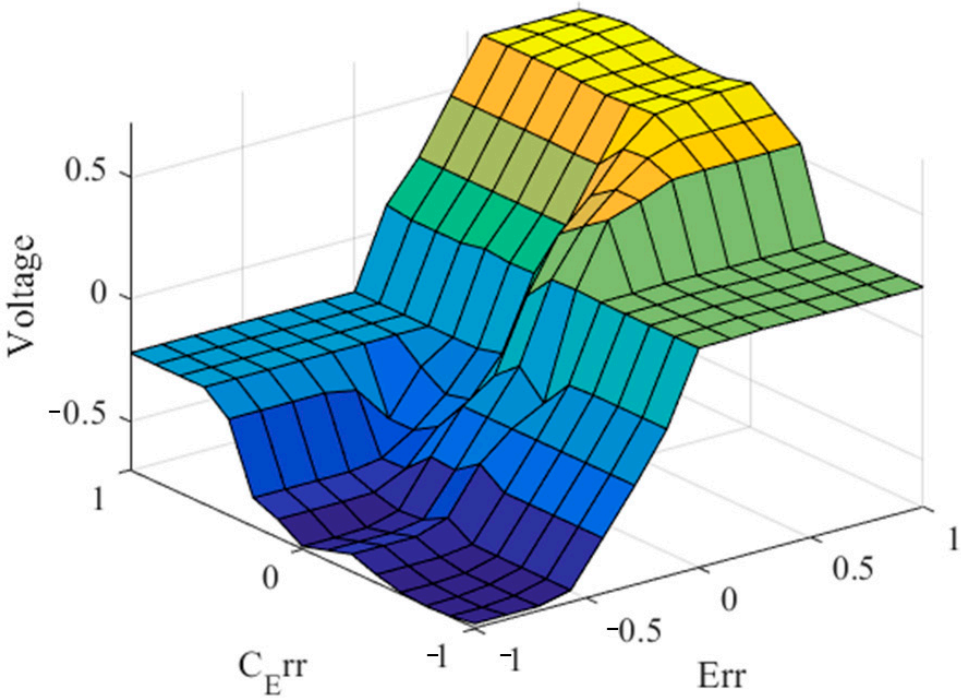

Figure 19. Surface using 0.05 URN noise.

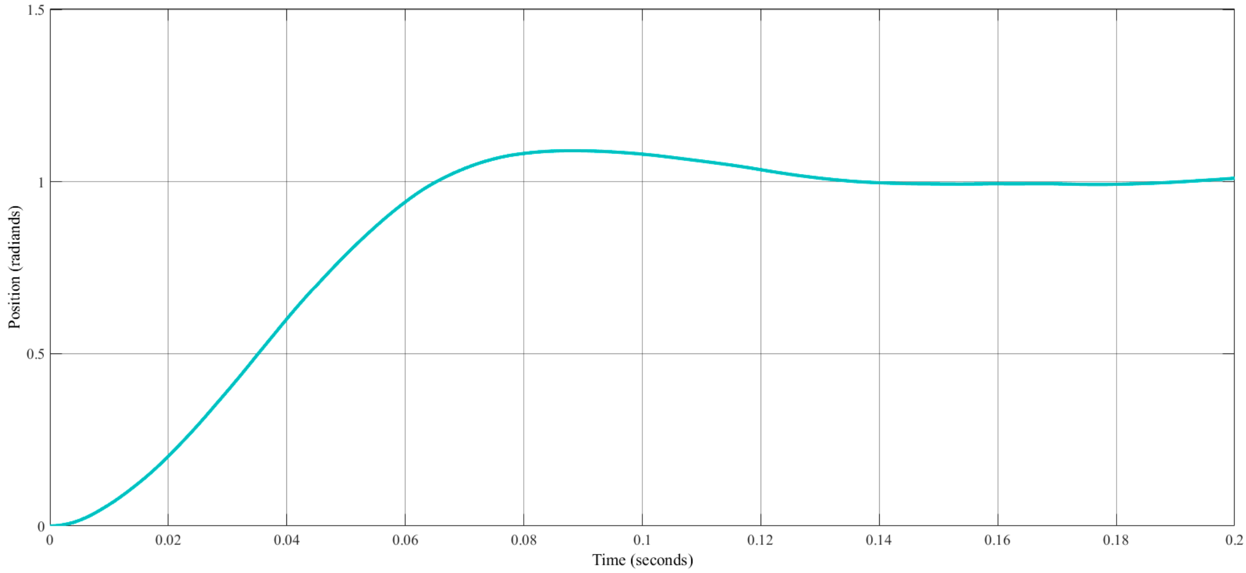

Figure 20. Controller reference using 0.06 noise.

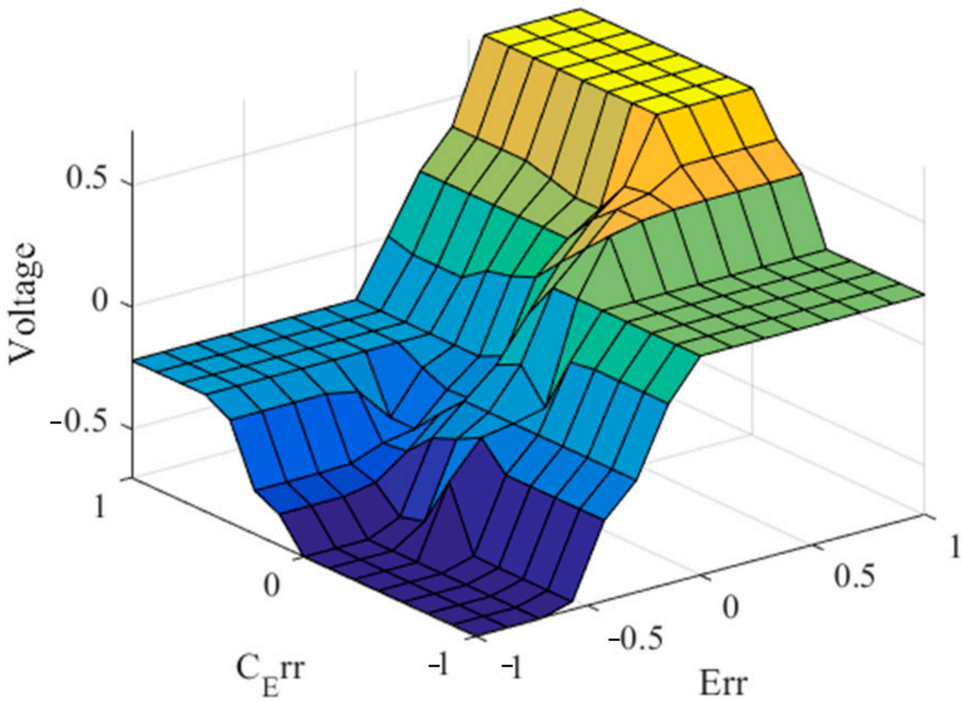

Figure 21. Surface using 0.06 URN noise.

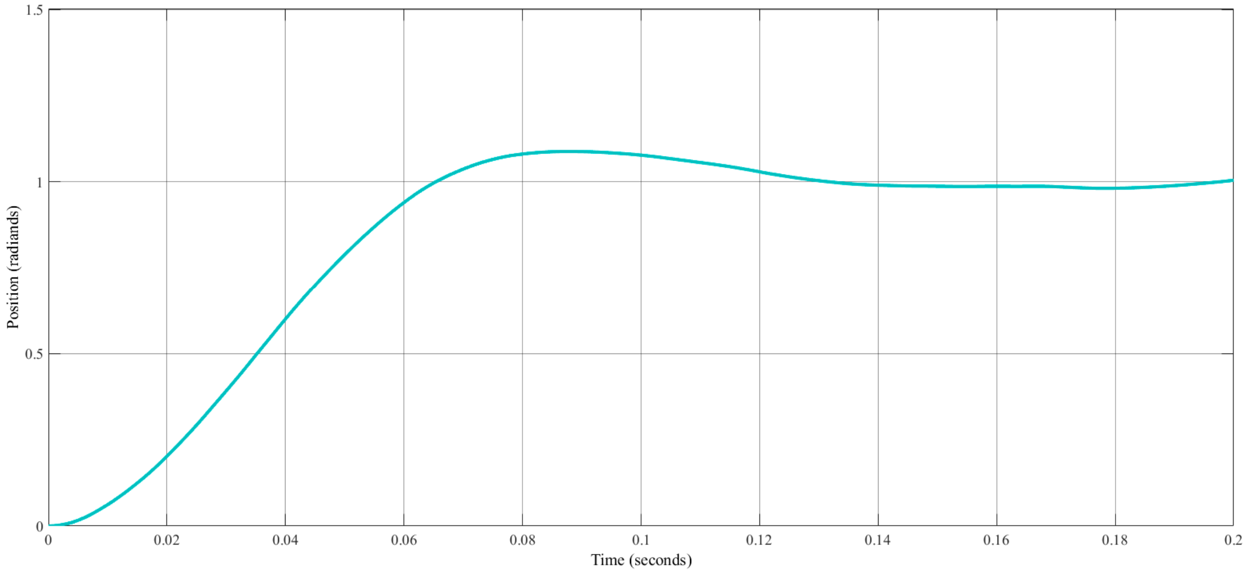

Figure 22. Controller reference using 0.07 noise.

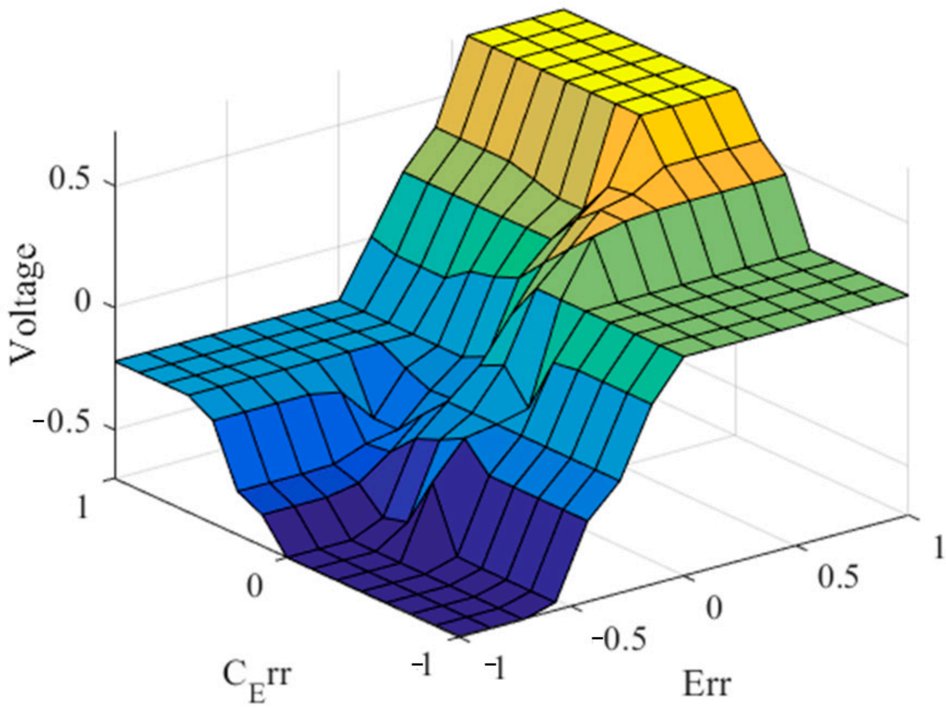

Figure 23. Surface using 0.07 URN noise.

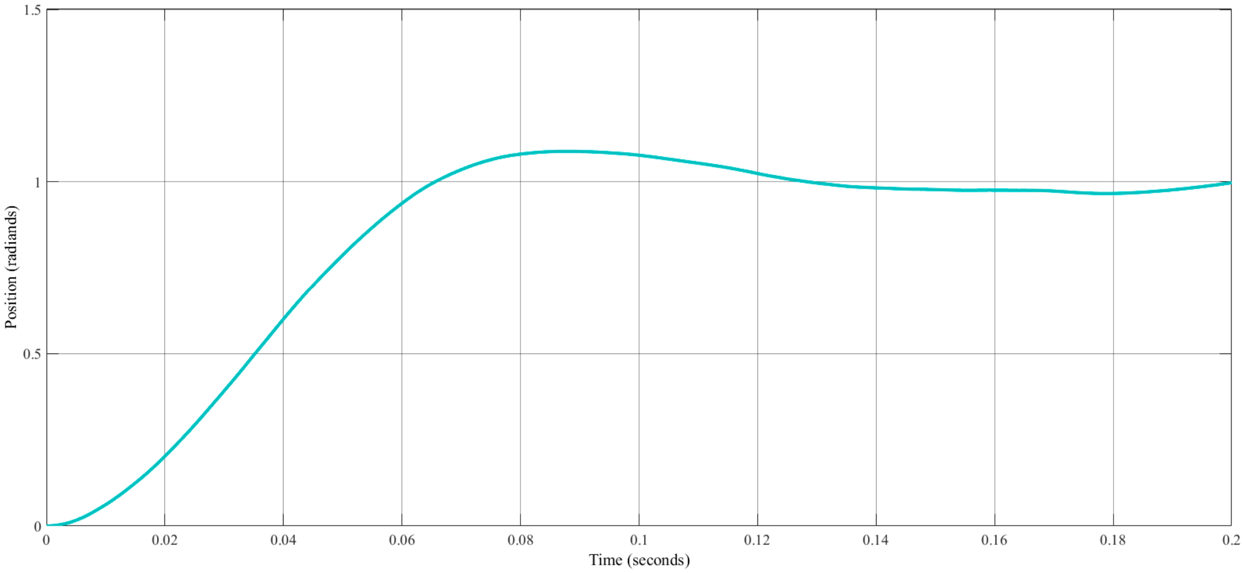

Figure 24. Controller reference using 0.08 noise.

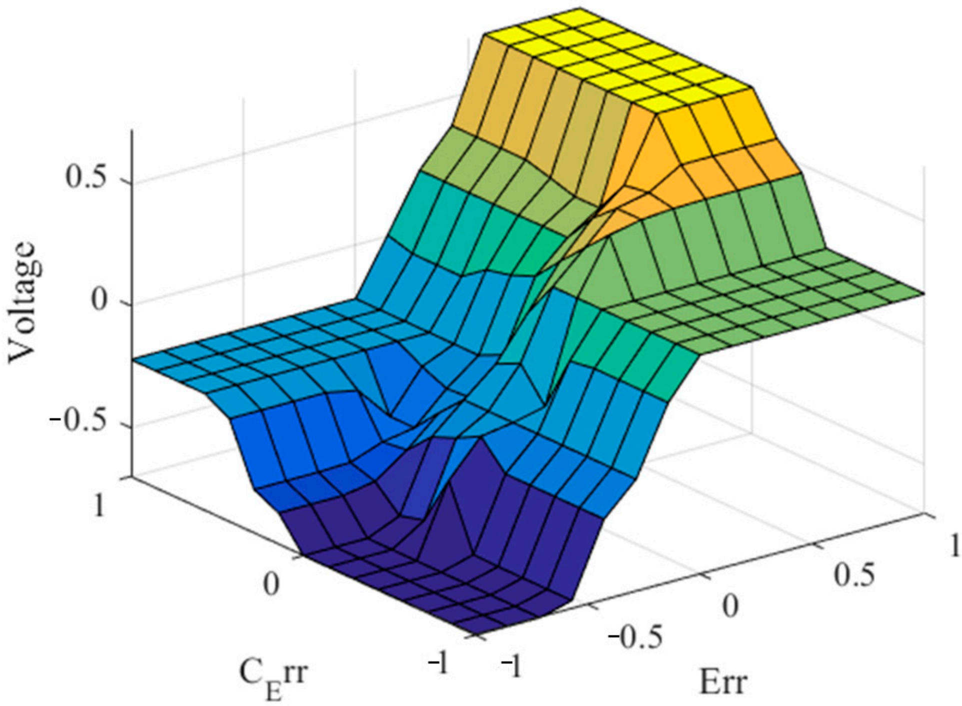

Figure 25. Surface using 0.08 URN noise.

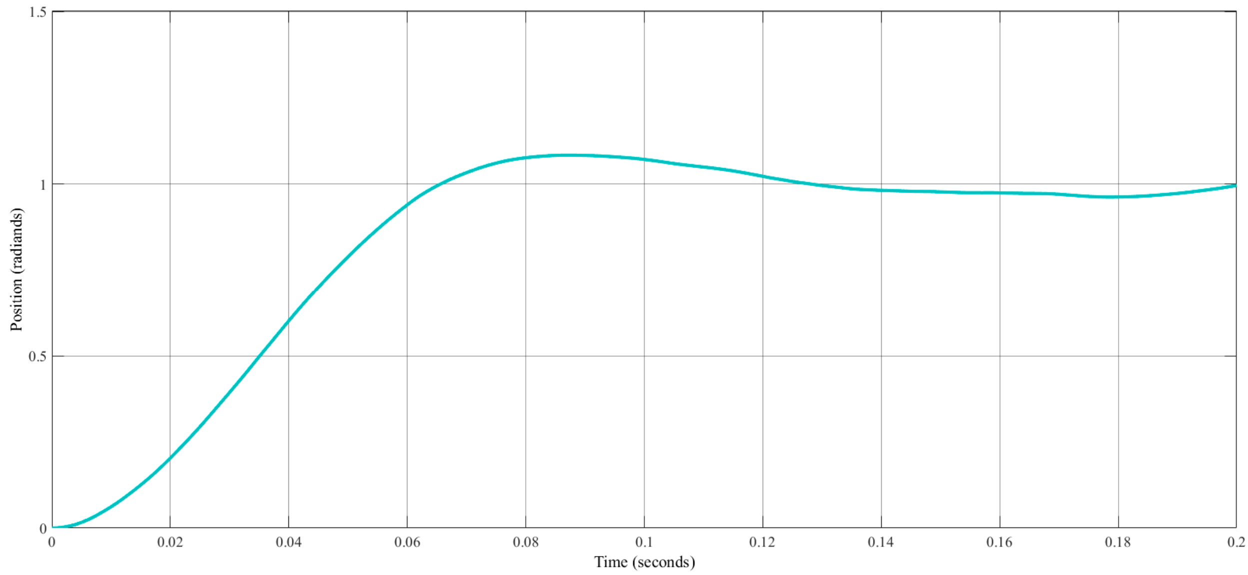

Figure 26. Controller reference using 0.09 noise.

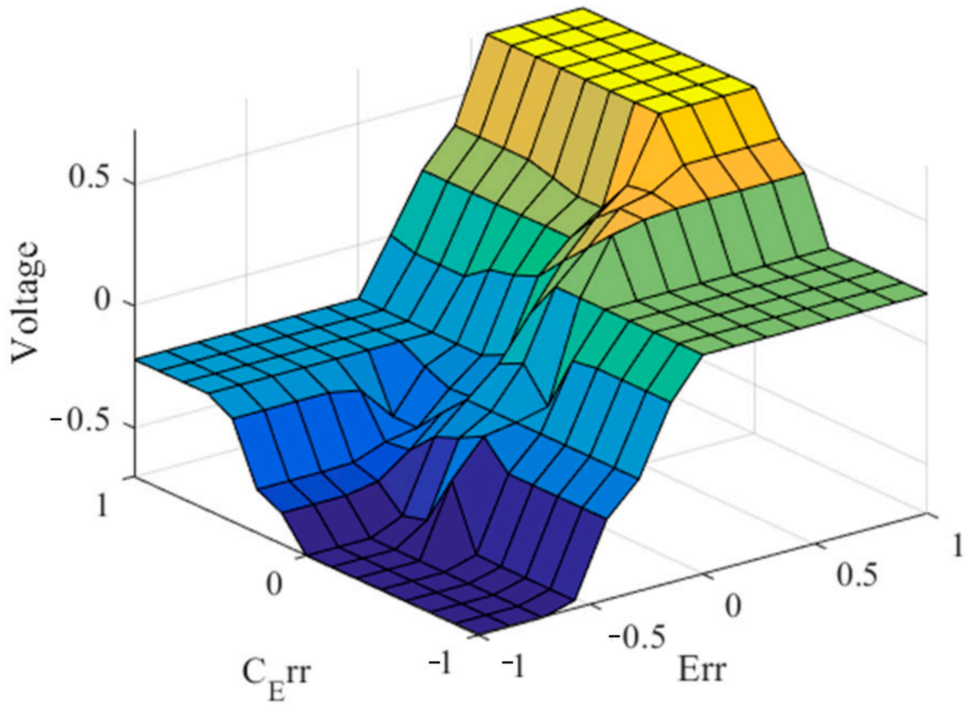

Figure 27. Surface using 0.09 URN noise.

7. Conclusions

This article introduces an innovative application of the type-2 fuzzy system theory with shadow sets, focusing on the utilization of only two alpha planes to address the challenge of reducing computational costs. The specific context of this application is the dynamic adaptation of the HMR parameter within the harmony search algorithm. Furthermore, the proposed methodology is implemented in an interval type-2 control problem to explore its effectiveness in handling increased uncertainty. The results obtained from simulations conducted with and without noise are presented and analyzed.

The analysis of the simulation results highlights a significant finding: the introduction of a noise level to the system leads to a reduction in the RMSE error. This observation is supported by the comparison of the obtained signals, which clearly demonstrate an improved performance when compared to the noise-free reference. As a result, it can be confidently concluded that the proposed approach exhibits a high efficiency in controlling angular position.

By utilizing only two alpha planes and incorporating shadow sets, the computational costs associated with the type-2 fuzzy system theory are effectively minimized. This reduction in the computational burden is crucial in addressing the complexity of control problems. The successful application of the proposed methodology not only offers a feasible solution to the interval type-2 control problem but also establishes the advantages of managing uncertainty through the integration of noise.

In conclusion, this research contributes to the field of control systems by presenting an innovative approach that combines the type-2 fuzzy system theory with shadow sets and dynamic parameter adaptation. Further research endeavors may explore the application of type-3 fuzzy controllers or extend the proposed methodology to different control problem domains. By continuing to explore and refine the approach, control systems can be further enhanced to tackle increasingly complex challenges in various industries and domains.

Author Contributions: C.P., P.O. and O.C. contributed to the literature review, software development, and validation. O.C. provided supervision, and P.M. contributed to the methodology. All authors have read and agreed to the published version of the manuscript.

Funding: This research did not receive any external funding.

Institutional Review Board Statement: Not Applicable.

Informed Consent Statement: Not Applicable.

Data Availability Statement: Not applicable.

Acknowledgments: We would like to express our gratitude to TecNM, Tijuana Institute of Technology.

Conflicts of Interest: The authors declare no conflict of interest.

References

1. Zimmermann, H.J. Fuzzy control. In *Fuzzy Set Theory—And Its Applications*; Springer: Dordrecht, The Netherlands, 2001; pp. 223–264. [CrossRef]
2. Sugeno, M. An introductory survey of fuzzy control. *Inf. Sci.* **1985**, *36*, 59–83. [CrossRef]
3. Zhang, H.; Liu, D. *Fuzzy Modeling and Fuzzy Control*; Springer Science & Business Media: Berlin/Heidelberg, Germany, 2006.
4. Precup, R.-E.; Hellendoorn, H. A survey on industrial applications of fuzzy control. *Comput. Ind.* **2011**, *62*, 213–226. [CrossRef]
5. Nguyen, A.-T.; Taniguchi, T.; Eciolaza, L.; Campos, V.; Palhares, R.; Sugeno, R.M. Fuzzy Control Systems: Past, Present and Future. *IEEE Comput. Intell. Mag.* **2019**, *14*, 56–68. [CrossRef]
6. Abdelrahim, E. Hierarchical Adaptive Genetic Algorithm Based T–S Fuzzy Controller For Non-linear Automotive Applications. *Int. J. Fuzzy Syst.* **2022**, *24*, 607–621. [CrossRef]
7. Liu, Z.; Yu, J.; Lam, H.-K. Passivity-Based Adaptive Fuzzy Control for Stochastic Nonlinear Switched Systems via T–S Fuzzy Modeling. *IEEE Trans. Fuzzy Syst.* **2022**, *31*, 1401–1408. [CrossRef]
8. Taghieh, A.; Mohammadzadeh, A.; Zhang, C.; Kausar, N.; Castillo, O. A type-3 fuzzy control for current sharing and voltage balancing in microgrids. *Appl. Soft Comput.* **2022**, *129*, 109636. [CrossRef]
9. Jahanshahi, H.; Yousefpour, A.; Soradi-Zeid, S.; Castillo, O. A review on design and implementation of type-2 fuzzy controllers. *Math. Methods Appl. Sci.* **2022**. [CrossRef]
10. Castillo, O.; Castro, J.R.; Melin, P. Interval Type-3 Fuzzy Control for Automated Tuning of Image Quality in Televisions. *Axioms* **2022**, *11*, 276. [CrossRef]
11. Ding, S.; Zhao, T.; Zhang, W.; Gao, F.; Zhu, B.; Tang, Z. Motion-inhibition control of a multi-robot mooring system using an actuating force fuzzy control method. *Ocean Eng.* **2023**, *267*, 113236. [CrossRef]
12. Liu, Y.; Zhu, Q.; Fan, X. Event-triggered adaptive fuzzy control for stochastic nonlinear time-delay systems. *Fuzzy Sets Syst.* **2023**, *452*, 42–60. [CrossRef]
13. Zandieh, F.; Ghannadpour, S.F. A comprehensive risk assessment view on interval type-2 fuzzy controller for a time-dependent HazMat routing problem. *Eur. J. Oper. Res.* **2023**, *305*, 685–707. [CrossRef]
14. Bostani, Y.; Jalilzadeh, S. A New Approach based on Wide-Area Fuzzy Controller for Damping of Sub Synchronous Resonance in Power System including DFIG. *J. Oper. Autom. Power Eng.* **2023**, *11*, 61–68. [CrossRef]
15. Batoo, K.M.; Pandiaraj, S.; Muthuramamoorthy, M.; Raslan, E.H.; Krishnamoorthy, S. Behavior-based swarm model using fuzzy controller for route planning and E-waste collection. *Environ. Sci. Pollut. Res.* **2022**, *29*, 19940–19954. [CrossRef] [PubMed]

16. Ha, S.; Chen, L.; Liu, H.; Zhang, S. Command filtered adaptive fuzzy control of fractional-order nonlinear systems. *Eur. J. Control.* **2022**, *63*, 48–60. [CrossRef]
17. Yao, Y.; Tan, J.; Wu, J.; Zhang, X. A Unified Fuzzy Control Approach for Stochastic High-Order Nonlinear Systems With or Without State Constraints. *IEEE Trans. Fuzzy Syst.* **2022**, *30*, 4530–4540. [CrossRef]
18. He, F.; Huang, Q. Time-Optimal Trajectory Planning of 6-DOF Manipulator Based on Fuzzy Control. *Actuators* **2022**, *11*, 332. [CrossRef]
19. Wang, Z.; Sun, K.; Ma, S.; Sun, L.; Gao, W.; Dong, Z. Improved Linear Quadratic Regulator Lateral Path Tracking Approach Based on a Real-Time Updated Algorithm with Fuzzy Control and Cosine Similarity for Autonomous Vehicles. *Electronics* **2022**, *11*, 3703. [CrossRef]
20. Abdenouri, N.; Zoukit, A.; Salhi, I.; Doubabi, S. Model identification and fuzzy control of the temperature inside an active hybrid solar indirect dryer. *Sol. Energy* **2022**, *231*, 328–342. [CrossRef]
21. Melin, P.; Ontiveros-Robles, E.; Gonzalez, C.I.; Castro, J.R.; Castillo, O. An approach for parameterized shadowed type-2 fuzzy membership functions applied in control applications. *Soft Comput.* **2019**, *23*, 3887–3901. [CrossRef]
22. Chatterjee, K.; De, A.; Chan, F.T. Real time traffic delay optimization using shadowed type-2 fuzzy rule base. *Appl. Soft Comput.* **2019**, *74*, 226–241. [CrossRef]
23. Patel, H.R.; Shah, V.A. General type-2 fuzzy logic systems using shadowed sets: A new paradigm towards fault-tolerant control. In Proceedings of the 2021 Australian & New Zealand Control Conference (ANZCC), Gold Coast, Australia, 25–26 November 2021; pp. 116–121. [CrossRef]
24. Gonzalez, C.I.; Melin, P.; Castillo, O.; Juarez, D.; Castro, J.R. Toward general type-2 fuzzy logic systems based on shadowed sets. In *Advances in Fuzzy Logic and Technology*; Springer: Cham, Switzerland, 2017; Volume 642, pp. 131–142. [CrossRef]
25. Linda, O.; Manic, M. Shadowed type-2 fuzzy sets-type-2 fuzzy sets with shadowed secondary membership functions. In Proceedings of the IEEE International Conference on Fuzzy Systems, Brisbane, Australia, 12–15 June 2012. [CrossRef]
26. Tahayori, H.; Sadeghian, A. Shadowed fuzzy sets: A framework with more freedom degrees for handling uncertainties than interval type-2 fuzzy sets and lower computational complexity than general type-2 fuzzy sets. *New Concepts Appl. Soft Comput.* **2013**, *854*, 97–117. [CrossRef]
27. Peraza, C.; Ochoa, P.; Castillo, O. Parameter Adaptation in Harmony Search with Shadowed Type-2 Fuzzy Approach for Designing Optimized Interval Type-2 Fuzzy Controllers. In Proceedings of the International Conference on Intelligent and Fuzzy Systems 2022, Izmir, Turkey, 19–21 July 2022; pp. 730–738. [CrossRef]
28. Kumar, P.; Dudeja, C. Shadowed type 2 fuzzy-based Markov model to predict shortest path with optimized waiting time. *Soft Comput.* **2021**, *25*, 995–1005. [CrossRef]
29. Tahayori, H.; Sadeghian, A. Handling uncertainties of membership functions with Shadowed Fuzzy Sets. In Proceedings of the World Automation Congress, Puerto Vallarta, Mexico, 24–28 June 2012.
30. Tahayori, H.; Sadeghian, A.; Pedrycz, W. Induction of shadowed sets based on the gradual grade of fuzziness. *IEEE Trans. Fuzzy Syst.* **2013**, *21*, 937–949. [CrossRef]
31. Khanduja, N.; Bhushan, B. Chaotic state of matter search with elite opposition based learning: A new hybrid metaheuristic algorithm. *Optim. Control. Appl. Methods* **2023**, *44*, 533–548. [CrossRef]
32. Arasteh, B. Clustered design-model generation from a program source code using chaos-based metaheuristic algorithms. *Neural Comput. Appl.* **2023**, *35*, 3283–3305. [CrossRef]
33. Goli, A.; Ala, A.; Hajiaghaei-Keshteli, M. Efficient multi-objective meta-heuristic algorithms for energy-aware non-permutation flow-shop scheduling problem. *Expert Syst. Appl.* **2023**, *213*, 119077. [CrossRef]
34. Gharehchopogh, F.S. Quantum-inspired metaheuristic algorithms: Comprehensive survey and classification. *Artif. Intell. Rev.* **2023**, *56*, 5479–5543. [CrossRef]
35. Azizi, M.; Talatahari, S.; Gandomi, A.H. Fire Hawk Optimizer: A novel metaheuristic algorithm. *Artif. Intell. Rev.* **2023**, *56*, 287–363. [CrossRef]
36. Zadeh, L.A. Fuzzy sets. *Inf. Control* **1965**, *8*, 338–353. [CrossRef]
37. Wagner, C.; Hagras, H. Toward General Type-2 Fuzzy Logic Systems Based on zSlices. *IEEE Trans. Fuzzy Syst.* **2010**, *18*, 637–660. [CrossRef]
38. Coupland, S.; John, R. Geometric Type-1 and Type-2 Fuzzy Logic Systems. *IEEE Trans. Fuzzy Syst.* **2007**, *15*, 3–15. [CrossRef]
39. Mendel, J.M.; Liu, F.; Zhai, D. α-Plane Representation for Type-2 Fuzzy Sets: Theory and Applications. *IEEE Trans. Fuzzy Syst.* **2009**, *17*, 1189–1207. [CrossRef]
40. Mendel, J.M.; John, R.I.; Liu, F. Interval Type-2 Fuzzy Logic Systems Made Simple. *IEEE Trans. Fuzzy Syst.* **2006**, *14*, 808–821. [CrossRef]
41. Wijayasekara, D.; Linda, O.; Manic, M. Shadowed Type-2 Fuzzy Logic Systems. In Proceedings of the IEEE Symposium on Advances in Type-2 Fuzzy Logic Systems (T2FUZZ), Singapore, 16–19 April 2013; pp. 15–22. [CrossRef]
42. Pedrycz, W. From fuzzy sets to shadowed sets: Interpretation and computing. *Int. J. Intell. Syst.* **2009**, *24*, 48–61. [CrossRef]
43. Pedrycz, W.; Song, M. Granular fuzzy models: A study in knowledge management in fuzzy modeling. *Int. J. Approx. Reason.* **2012**, *53*, 1061–1079. [CrossRef]
44. Pedrycz, W.; Vukovich, G. Granular computing in the development of fuzzy controllers. *Int. J. Intell. Syst.* **1999**, *14*, 419–447. [CrossRef]

45. Geem, Z.W. State-of-the-Art in the Structure of Harmony Search Algorithm. In *Recent Advances in Harmony Search Algorithm*; Springer: Berlin/Heidelberg, Germany, 2010; Volume 270, pp. 1–10. [CrossRef]
46. Geem, Z.W.; Choi, J.-Y. Music Composition Using Harmony Search Algorithm. In *Applications of Evolutionary Computing*; Giaco-bini, M., Ed.; Springer: Berlin/Heidelberg, Germany, 2007; Volume 4448, pp. 593–600.
47. Lee, K.S.; Geem, Z.W. A new meta-heuristic algorithm for continuous engineering optimization: Harmony search theory and practice. *Comput. Methods Appl. Mech. Eng.* **2005**, *194*, 3902–3933. [CrossRef]
48. Kim, J.H.; Lee, H.M.; Yoo, D.G. Investigating the Convergence Characteristics of Harmony Search. In *Harmony Search Algorithm*; Springer: Berlin/Heidelberg, Germany, 2016; Volume 382, pp. 3–10. [CrossRef]
49. Abdulkhaleq, M.T.; Rashid, T.A.; Alsadoon, A.; Hassan, B.A.; Mohammadi, M.; Abdullah, J.M.; Chhabra, A.; Ali, S.L.; Othman, R.N.; Hasan, H.A.; et al. Harmony search: Current studies and uses on healthcare systems. *Artif. Intell. Med.* **2022**, *131*, 102348. [CrossRef] [PubMed]
50. Abu Doush, I.; Al-Betar, M.A.; Awadallah, M.A.; Alyasseri, Z.A.A.; Makhadmeh, S.N.; El-Abd, M. Island neighboring heuristics harmony search algorithm for flow shop scheduling with blocking. *Swarm Evol. Comput.* **2022**, *74*, 101127. [CrossRef]
51. Ocak, A.; Nigdeli, S.M.; Bekdaş, G.; Kim, S.; Geem, Z.W. Optimization of Seismic Base Isolation System Using Adaptive Harmony Search Algorithm. *Sustainability* **2022**, *14*, 7456. [CrossRef]
52. Kayhan, A.H.; Demir, A.; Palanci, M. Multi-functional solution model for spectrum compatible ground motion record selection using stochastic harmony search algorithm. *Bull. Earthq. Eng.* **2022**, *20*, 6407–6440. [CrossRef]
53. Jahjouh, M.; Erhan, S. Optimization of prestressed concrete bridge girder section using a modified harmony search algorithm. *Structures* **2022**, *46*, 625–636. [CrossRef]
54. Santos, J.D.; Marques, F.; Negrete, L.P.G.; Brigatto, G.A.A.; López-Lezama, J.M.; Muñoz-Galeano, N. A Novel Solution Method for the Distribution Network Reconfiguration Problem Based on a Search Mechanism Enhancement of the Improved Harmony Search Algorithm. *Energies* **2022**, *15*, 2083. [CrossRef]
55. Gupta, S. Enhanced harmony search algorithm with non-linear control parameters for global optimization and engineering design problems. *Eng. Comput.* **2022**, *38*, 3539–3562. [CrossRef]
56. Zhang, Y.; Li, J.; Li, L. A Reward Population-Based Differential Genetic Harmony Search Algorithm. *Algorithms* **2022**, *15*, 23. [CrossRef]

Disclaimer/Publisher's Note: The statements, opinions and data contained in all publications are solely those of the individual author(s) and contributor(s) and not of MDPI and/or the editor(s). MDPI and/or the editor(s) disclaim responsibility for any injury to people or property resulting from any ideas, methods, instructions or products referred to in the content.